OXIDATIVE BIOCATALYSIS WITH NOVEL NADH OXIDASES

A Thesis
Presented to
The Academic Faculty

by

Rongrong Jiang

In Partial Fulfillment
of the Requirements for the Degree
Doctor of Philosophy in the
School of Chemical & Biomolecular Engineering

Georgia Institute of Technology
August 2006

OXIDATIVE BIOCATALYSIS WITH NOVEL NADH OXIDASES

Approved by:

Dr. Andreas S. Bommarius, Advisor
School of Chemical & Biomolecular Engineering
Georgia Institute of Technology

Dr. Dale E. Edmondson
Department of Biochemistry
Emory University

Dr. Ronald W. Rousseau
School of Chemical & Biomolecular Engineering
Georgia Institute of Technology

Dr. David Rozzell
Biocatalytics, CA

Dr. Athanassios Sambanis
School of Chemical & Biomolecular Engineering
Georgia Institute of Technology

Date Approved: June 21, 2006

To my parents

ACKNOWLEDGEMENTS

First of all, I would like to thank Andy, my advisor, for his continuous help and support through my graduate studies here at Georgia Tech. I could not have achieved what I have achieved today without his encouragement. I am also grateful to my thesis committee members: Dr. Dale E. Edmondson, Dr. Allen M. Orville, Dr. David Rozzell, Dr. Ronald W. Rousseau and Dr. Athanassios Sambanis for their time and advice. Special thanks to Dr. Dale E. Edmondson, who agrees to serve on my committee on such a short notice.

I would also like to thank the members in my group: Tracey Thaler, Javier Chaparro-Riggers, Karen Polizzi, James Broering, Bernard Loo, Phillip Gibbs, Eduardo Vazquez-Figueroa, Thomas Rogers, Anshul Dubey and Jana Billy for their help and enthusiastic discussion throughout my research, especially Thomas Rogers, who helped set up the enzyme membrane reactor.

The members of Atlanta Flavin Group: Dr. Giovanni Gadda, and Dr. Min Li are also deserving of my deepest thanks. Their advice was the light guiding me through the difficulties dealing with flavoproteins.

I would like to thank Brian Lynch in the School of Biology at Georgia Tech and Perry Mars of the Fundamental and Applied Molecular Evolution (FAME) sequencing center at Emory University for providing sequencing results.

Last but not least, I would like to thank my friends and family. Without my parents' love and support, I would not be able to finish my studies here and this is for them. My best friends, Ding Dang, Na Yang, Manish Gupta, Qinyi Wu and Yi Zhang are

always on my side through thick and thin. Uncle Charlie Jiang, my only relative in US, helped me through the toughest time in my life. I couldn't have finished this without them.

TABLE OF CONTENTS

LIST OF TABLES

LIST OF FIGURES

ABBREVIATIONS

L-GluDH	L-Glutamate Dehydrogenase
AhpR	Alkyl hydroperoxide reductase
Nox-2	Water-forming NADH oxidase
L. sanfranciscensis	*Lactobacillus sanfranciscensis*
L.san-Nox2	Water-forming NADH oxidase from *Lactobacillus sanfranciscensis*
L.lac-Nox2	Water-forming NADH oxidase from *Lactococcus lactis*
L. lactis	*Lactococcus lactis*
CR	Carbonyl reductase
LL-CR	Carbonyl reductase from *Lactococcus lactis*
LeuDH	Leucine dehydrogenase
PMS	Phenzaine methodsulfate
LDH	Lactate deydrogenase
ADH	Alcohol dehydrogenase
HL-ADH	Horse-liver alcohol dehydrogenase
Prxs	Peroxiredoxins
S. mutans	*Sreptococcus mutans*
AhpC	Peroxidase gene
Nox-1	Hydrogen peroxide forming NADH oxidase
AhpF	Hydrogen peroxide forming NADH oxidase gene
noxE	Water-forming NADH oxidase gene from *Lactococcus lactis*
*A. xylan*us	*Amphibacillus xylanus*

S. typhymurium	*Salmonella typhymurium*
NTD	N-terminal redox-active disulfide-containing domain
NADH/SS	NADH binding redox-active disulfide-containing domain
TrxR	Thioredoxin reductase
Trx	Thioredoxin
TTN	Total turnover number
S. A.	Specific activity
NADH	Nicotinamide adenine dinucleotide, reduced
NAD^+	Nicotinamide adenine dinucleotide
$NADP^+$	Nicotinamide adenine dinucleotide phosphate
NADPH	Nicotinamide adenine dinucleotide phosphate, reduced
ADP	Adenosine diphosphate
FAD	Flavin adenine dinucleotide
COBE	Ethyl 4-chloro-3-oxobutanoate
CHBE	Ethyl-4-chloro-3-hydroxybutanoate
GDH	Glucose dehydrogenase
AR	Aldehyde reductase
pNC	pETDuet-1 vector with *L.san*-Nox2 gene first and LL-CR second
pCN	pETDuet-1 vector with LL-CR gene first and *L.san*-Nox2 second
GC	Gas Chromatography
IPTG	Isopropyl ß–D-thiogalactopyranoside
GC-FID	Gas Chromatography-flame ionization detector
DTT	Dithiothreitol

MWCO	Molecular weight cut off
EMR	Enzyme membrane reactor
CSTR	Continuously stirred tank reactor
FDH	Formate dehydrogenase
CLECs	Cross-linked enzyme crystals
MDMA	3, 4-methylenedioxymethamphetamine

SUMMARY

Many oxidoreductases need nicotinamide cofactors for their reactions. The big obstacle of using these syntheses in industry is the high cost of these nicotinamide cofactors. The work here is about finding novel NADH oxidases from *Lactococcus lactis* and applying in a cofactor regeneration system with carbonyl reductase or alcohol dehydrogenase. NADH oxidases are useful biocatalysts for regenerating nicotinamide cofactors of biological redox reactions. The annotated alkyl hydroperoxide reductase (AhpR) and the H_2O-forming enzyme (nox-2) genes from *Lactococcus lactis* (*L. lactis, L.lac*-Nox2) were cloned and proteins were expressed and characterized. They were compared with the H_2O-former from *Lactobacillus sanfranciscensis* (*L. sanfranciscensis, L.san*-Nox2). AhpR is composed of H_2O_2-forming NADH oxidase (nox-1) and peroxidase and the net reaction of AhpR is the same as nox-2 when oxygen is the substrate. Both nox-1 and nox-2 are flavoproteins and turnover-limited. In the absence of exogenously added thiols, both nox-1 and nox-1/peroxidase are considerably more stable against overoxidation than nox-2. *L.san*-Nox2 was crystallized and was found to have ADP ligand, but according to the HPLC results, no ADP ligand was found in the *L. lac*-Nox-2. Enzyme membrane reactor was used for the application of oxidative reaction of cyclohexanol to cyclohexanone, with isolated enzymes horse liver alcohol dehydrogenase and *L.lac*-Nox2.

CHAPTER 1

INTRODUCTION

The interest in using enzymatic transformations in industrial processes continues to grow rapidly. Among the enzymes for potential application, hydrolases and oxidoreductases are the most prominent categories. Many oxidoreductases need nicotinamide cofactors for their reactions and some of them are applied on large scale in industry. One obstacle of applying these syntheses in industry is the high cost of the nicotinamide cofactors. The solution is to use the *in situ* cofactor regeneration system. The work here is about finding novel NADH oxidases for the NAD^+ regeneration and applying them in the cofactor regeneration system with carbonyl reductase and alcohol dehydrogenase.

Chapter 2 is focusing on the background of cofactor regeneration. Nicotinamide cofactors are widely used as electron carriers among many biochemical reactions. $NAD(P)^+$ are needed in oxidative reactions and NAD(P)H are needed in reductive reactions. For example, in Figure 1.1, L-Glutamate Dehydrogenase (L-GluDH) catalyzes the reductive reaction and needs NAD^+ as its cofactor. There are two categories of cofactor regeneration: NAD(P)H regeneration and $NAD(P)^+$ regeneration. Regeneration of reduced nicotinamide cofactors NAD(P)H from $NAD(P)^+$ has been well studied. Alcohol dehydrogenase, formate dehydrogenase, amino acid dehydrogenase, phosphite dehydrogenase and hydroxy acid dehydrogenase were investigated for that purpose. On

the other hand, the regeneration of $NAD(P)^+$ from NAD(P)H was less well studied. In this work, my focus will be the regeneration of $NAD(P)^+$ cofactors. The cofactor could be regenerated biologically, chemically, photo-chemically and electrochemically. But the criterion of high reaction rate and turnover number eliminates all of the methods except the biological method, i.e., using enzymes to regenerate $NAD(P)^+$. NADH oxidase is a good choice for this purpose. NADH oxidase uses oxygen as its substrate and would not generate by-products to inhibit the enzymes involved. The reaction of water-forming NADH oxidase is an irreversible one, so when it is coupled with a reversible reaction, it will drive the equilibrium towards the formation of the product. There are two categories of NADH oxidase: 1) hydrogen-peroxide forming NADH oxidase (nox-1) 2) water-forming NADH oxidase (nox-2).

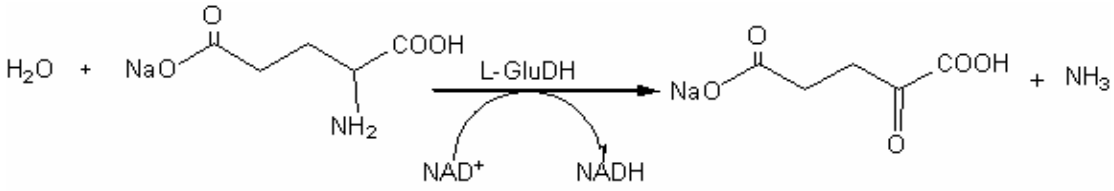

Figure 1.1: L-GluDH catalyzes the oxidative reaction of mono-sodium glutamate

Chapter 3 is about the alkyl hydroperoxide reductase from *L. lactis*. Alkyl hydroperoxide reductase is composed of two enzymes: nox-1 and peroxidase (AhpC). The overall reaction of alkyl hydroperoxide reductase (AhpR) is the same as nox-2 (nox-1: $O_2 + NADH + H^+ \longrightarrow NAD^+ + H_2O_2$; nox-2: $O_2 + 2\ NADH + 2\ H^+ \longrightarrow 2\ NAD^+ + 2\ H_2O$), with oxygen as the substrate. Alkyl hydroperoxide reductase is a category of non-heme, non-selenium proteins in lactic acid bacteria for the defense against peroxide

during metabolism. Both the annotated nox-1 and AhpC from *L. lactis* have high amino acid similarity with other nox-1s and AhpCs from other lactic acid bacteria. In Chapter 3, the process of AhpR (*L. lactis*) cloning, overexpression and characterization were described in details.

After characterizing AhpR from *L. lactis*, the water-forming NADH oxidase was also cloned and characterized. Water-forming NADH oxidase is part of the oxygen defense system. It has been found in *Streptococcus pyogenes*, *Streptococcus mutans* and other bacteria. In chapter 4, the *L.lac*-Nox2 was characterized. Because both AhpR and *L.lac*-Nox2 conduct the same reaction when oxygen is the substrate, they were compared together with regards to specific activity and total turnover number. *L.lac*-Nox2 was also compared with the nox-2 found in *Lactobacillus sanfranciscensis*.

Chapter 5 covers *E. coli* whole-cell catalyst, containing both the carbonyl reductase gene from *Lactococcus lactis* (LL-CR) and the *L.san*-Nox2 gene, to oxidize 2-hexanol to 2-hexanone with the *in situ* cofactor regeneration system. Whole-cell catalysts have been used in industry thanks to their ease of handling. The recombinant DNA technique has greatly increased the availability of whole-cell catalyst. pETDuet vector and pACYCDuect vector were employed for the cloning of LL-CR gene and *L.san*-Nox2 gene in the two-plasmid-two-gene system and one-plasmid-two-gene system. Whereas the NAD(P)H cofactor regeneration in the whole-cell catalyst has been well investigated, the $NAD(P)^+$ regeneration is less well studied.

While chapter 5 covers using the whole-cell as catalyst for the cofactor regeneration, in Chapter 6, using isolated enzymes for the cofactor regeneration system in an enzyme membrane reactor (EMR) was investigated. The crucial advantage of enzyme

membrane reactor is the absence of mass transfer limitations compared to the immobilized enzyme. EMR is operated as a continuously stirred tank reactor and the operational stability of involved enzymes is the focus of our study. Two enzymes: horse liver alcohol dehydrogenase (HL-ADH) and *L.lac*-Nox2 are coupled for the oxidation of cyclohexanol. Horse-liver alcohol dehydrogenase is a well-investigated NAD^+-dependent enzyme that catalyzes the oxidation of primary and secondary alcohols and the reduction of aldehydes and ketones with relatively broad specificity. *L.lac*-Nox2 is here for the regeneration of NAD^+.

CHAPTER 2

BACKGROUND

Many oxidoreductases need nicotinamide cofactors for their reactions and some of them were applied in large scale in industry. For example, Eli Lilly and Company (Indianapolis, IN) developed a whole-cell biotransformation using dehydrogenase to reduce a prochiral ketone 3,4-methylenedioxyacetophenone to an optically active secondary alcohol—(S)-(3,4-methylenedioxy-phenyl)-2-propanol, which is an important intermediate for drug 3,4-methylenedioxymethamphetamine (MDMA) (Figure 2.1). NADH is the cofactor for the dehydrogenase (2).

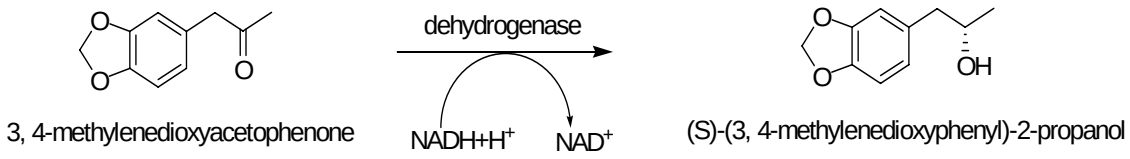

Figure 2.1: Reduction of 3, 4-mthylenedioxyacetophenone with dehydrogenase

Leucine dehydrogenase (LeuDH) also needs NADH as its cofactor. More than ten years ago, a process with continuous cofactor regeneration using isolated enzymes was developed. The reductive amination of trimethylpyruvate to L-tert-leucine was achieved using leucine dehydrogenase and formate dehydrogenase (FDH). Formate dehydrogenase serves to regenerate NADH for the production reaction (Figure 2.2). This process has now reached ton-scale (3) .

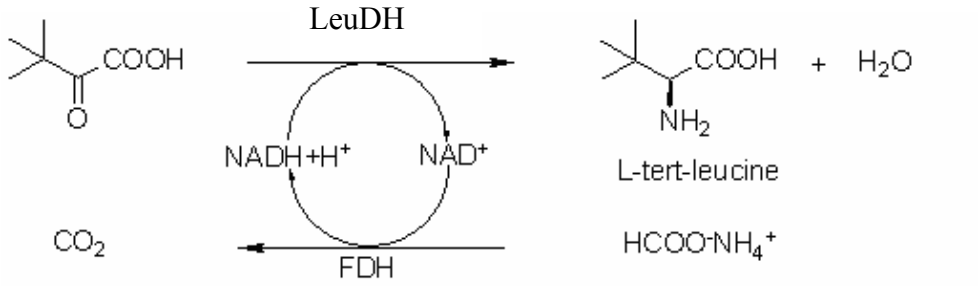

Figure 2.2: L-tert-leucine production with cofactor regeneration system.

2.1 Nicotinamide cofactors

Nicotinamide cofactors are widely used as electron carriers among many biochemical reactions. There are two categories of nicotinamide cofactors: the oxidized form $NAD(P)^+$ and the reduced form NAD(P)H.

Both forms of nicotinamide cofactors are subject to decomposition in aqueous solution. In acid, the decomposition of NAD(P)H involves cyclization, epimerization and hydration (4). The order of events depends upon the pH and buffer concentration (5). The most effective general acid decomposition of NAD(P)H happens when those buffers whose pKas are approximately equal to the pH of the solution, except inorganic phosphate, HEPES, triethanolamine and Tris buffers. In base, the decomposition of $NAD(P)^+$ involve the hydrolysis of the nicotinamide ribose bond or nucelophilic addition to the nicotinamide ring (6-8). NAD(P)H is stable in base but labile in acid; $NAD(P)^+$ is stable in acid but labile in base (9,10). $NAD(P)^+$ can be destroyed by heating to 100 ºC at pH 11 for 15 min or in 0.1 M NaOH for 5 min (11), but NAD(P)H could bear heating at 100 ºC in 0.1 M NaOH for 30~60 min (12,13). However, prolonged storage in base does tend to promote the oxidation of NAD(P)H to $NAD(P)^+$ (9). In a coupled enzyme reaction, nicotinamide cofactor cycles between its oxidized and reduced forms.

2.1.1 Enzyme degradation of nicotinamide cofactors

In some enzyme preparations, phophodiesterases and phosphatases could show up as the impurities and would degrade NAD(P)(H) (14). Other enzymes, for example, NAD^+ pyrophosphatase, NAD^+ glycohydrolase and NAD^+ kinase, could degrade and transform NAD(P)(H) (15). In addition, nucleophilic additions to NAD^+ could be catalyzed by the following dehydrogenases: Lactate dehydrogenase catalyzes the addition of hydroxylamine or cyanide (16,17), sulfite (18); malate dehydrogenase catalyzes the addition of sulfite (18); horse liver alcohol dehydrogenase catalyzes the addition of hydroxylamine or cyanide (19).

2.1.2 Reduction potentials of nicotinamide cofactors

At pH 7.0, the generally accepted reduction potential ($2e^{-1}$) for the reduction of NAD^+ to NADH at 20 ºC is: E_0 = -0.32 V (20); that of $NAD(P)^+$ to NADPH is E_0 = -0.324 V (21) (all concentrations are 1 M except $[H^+] = 10^{-7}$ M). The potential changes as the pH and temperature changes.

2.2 Problems of using cofactor-requiring oxidoreductases

Although the oxidoreductases have been prepared and analyzed in the laboratory, the large-scale application is not common. One problem is that many oxidoreductases are multimeric when active (22,23). Their activity in solution or on supports requires the correct secondary and tertiary structures and proper interactions between subunits. Although improvements of stability have been achieved through protein engineering among some enzymes (24-28), further improvements are still in required. Oxidoreductases can be inactivated by oxidants and reductants in the solution, which are

very often present in the biochemical redox reactions. A second problem is that oxidoreductases show more complex kinetics behavior than those of hydrolases and isomerases, such as allosteric effects and noncompetitive product inhibition, which are particularly important (29). One fundamental reason is the high cost of the nicotinamide cofactors. It is too expensive to use it as a stoichiometric reagent, for example, NADH is \$67/g and NAD^+ is \$90/g from Sigma Aldrich. The cost of NAD(H)/$NAD(P)^+$ is the obstacle for large-scale application of nicotinamide cofactor-dependent enzyme, so the cofactor regeneration becomes very important. The way to reduce the cofactor costs in industry is to use the effective *in situ* cofactor regeneration systems.

Cells provide the cofactor for the oxidoreductases during fermentation. The nicotinamide cofactors are synthesized and regenerated inside the cell through cellular metabolism. When using isolated enzymes *in vitro*, nicotinamide cofactors must be regenerated separately. In addition to the system of production with oxidoreductases, a second system--cofactor regeneration--must be used.

2.3 Cofactor regeneration effects

Cofactor regeneration can accomplish three objectives in addition to reducing the cost of the cofactor(30). First of all, if irreversible, it can be used to affect the position of the coupled equilibrium. Cofactor regeneration couples to substrate formation and often shifts the overall equilibrium favorably towards product formation . For example, at pH 7.0, the equilibrium for the oxidation of sorbitol to fructose by NAD^+ strongly favors the formation of sorbitol and NAD^+ (31).

However, if lactate dehydrogenase is applied for the regeneration of NAD^+, it increases the equilibrium constant and drives the reaction towards the fructose and lactate

formation direction (32). Thus, cofactor regeneration reaction coupling with the production reaction favors the production formation.

Second of all, cofactor regeneration can obviate the problem of product inhibition from the cofactor produced by the synthetic reaction. Cofactor regeneration prevents the accumulation of cofactor by-product by reducing to a catalytic quantity of cofactor required and by consuming the cofactor produced by the synthetic reaction as it forms. Third, by eliminating the need for stoichimetric quantities of NAD(H), cofactor regeneration can simplify the reaction work-up.

2.4 Criteria of choosing cofactor regeneration system

The method to regenerate nicotinamide cofactors should be inexpensive, practical and convenient. The reaction for regeneration should have high yield and total turnover number (TTN). The total turnover number characterizes the enzyme operational stability: it is the total amount of product that an enzyme produces during its lifetime. To be useful, TTN of a regeneration system should be at least 10, 000 to 100,000. This will reduce the price of recycling cofactor to the level of 10~20 cents/cycle. The cofactor regeneration reaction should favor product production thermodynamically and kinetically. There should be a straightforward analysis method available for monitoring the process of the reaction. Last but not least, the cofactor should be active under operating conditions with whatever method is chosen.

There are two categories of nicotinamide cofactor regeneration: one is the regeneration of reduced nicotinamide cofactors NAD(P)H and the other is the regeneration of oxidized form $NAD(P)^+$.

2.5 Regeneration of reduced nicotinamide cofactors: NAD (P)$^+$ to NAD(P)H

Regeneration of the reduced forms of the pyridine nucleotide cofactors has been well studied. Alcohol dehydrogenases (ADHs), formate dehydrogenase, amino acid dehydrogenases, phosphite dehydrogenase and hydroxy acid dehydrogenases were studied for the regeneration of NAD(P)H (33-37). Horse-liver alcohol dehydrogenase (HL-ADH) and ADH from *Lactobacillus brevis* have been reported that can operate at reasonably high alcohol concentration and the TTN for the cofactor reached up to 20,000 (38).

The wild-type formate dehydrogenase from *Candida boidinii* has been applied successfully in industry for the production of L-tert-leucine at Degussa, but its low specific activity (6 U/mg) has been a limiting factor (39). L-tert-leucine was reported to be produced continuously in a membrane reactor with LeuDH and formate dehydrogenase with the total turnover number of 125, 000 (40).

A recently developed new enzyme, phosphite dehydrogenase, can also be used for NADH regeneration. It catalyzes the NAD^+-dependent oxidation of phosphite to phosphate. The specific activity of the enzyme is about 6 U/mg, with K_M values of 50 μM for both NAD^+ and phosphite (33,37).

2.6 Regeneration of oxidized nicotinamide cofactors: NAD(P)H to NAD(P)$^+$

Whereas regeneration of the reduced forms of the pyridine nucleotide cofactors has been extensively investigated, recycling of NAD(P)$^+$ from NAD(P)H has been less well studied. The motivation for NAD(P)$^+$ regeneration stems from the potential to either use dehydrogenase to resolve racemic mixtures of chiral alcohols and amines by

oxidizing one of the two enantiomers or to synthesize ketones that are difficult to prepare chemically. This work is going to focus on finding novel enzymes for the regeneration of the oxidized form cofactor NAD^+ and apply the novel enzyme in cofactor regeneration system. The $NAD(P)^+$-linked oxidative reactions usually have the problems such as unfavorable thermodynamics and product inhibition. The nicotinamide cofactor could be regenerated biologically, chemically, photo-chemically, electrochemically.

2.6.1 Electrochemical methods

The direct anodic oxidation of NAD(P)H is far more successful than direct electrochemical reduction of $NAD(P)^+$. The NADH oxidized at carbon or platinum electrodes yields cofactor that is 90-99% enzymatically active (41-43). Surface modification, such as the adsorption of aromatic alcohols or the covalent immobilization of LDH onto electrodes, improve the electrochemical activity of NAD(H) (44,45). The continuous electrochemical regeneration of NAD^+ has been demonstrated in reactors oxidizing ethanol to acetaldehyde (42).

The obstacle of using this method is electrode fouling by adsorbed components of the solution, including cofactor (46,47). Dye-mediated electron transfer between NAD(P)H and the anode might minimize the interaction of cofactor with the electrode.

2.6.2 Chemical and photochemical methods

Jones and Taylor developed a method to regenerate NAD^+: flavin mononucleotide (FMN) oxidizes NADH, and the reduced $FMNH_2$ is reoxidized *in situ* by reaction with oxygen. This system is very simple. It does not require the enzyme addition and FMN is commercially available. The major disadvantage is that the reaction of FMN with NADH is slow (29). The small rate constant for the reaction of FMN with NADH requires that

the two species be used in such high concentrations that FMN is typically present at concentrations similar to that of the reactant and the total turnover number does not exceed 25. FMN itself is very expensive and light sensitive, so the whole process will be expensive. FMN reductase, which catalyze the reduction of FMN was tried out to improve the regeneration system (48,49).

Other electron-transfer dyes, such as MB, DCPIP (light sensitive, reacts with thiol groups), phenazine methodsulfate (PMS), and potassium ferricyanide react faster than FMN, directly to oxidize NAD(P)H. PMS reacts with NADH most rapidly among all of these choices. However, the DCPIP and potassium ferricyanide cannot be oxidized by oxygen, so they are not suitable for the purpose of regeneration. The PMS can be reoxidized by oxygen and it is used to regenerate NAD^+ in many analytical procedures such as recycling NAD^+ in small-scale of oxidation of ethanol (50,51). But PMS is not stable—it reacts with oxygen and forms 2-keto-N-methylphenazine and phenazine.

Photoexcitation increases the rates of NAD(P)H oxidation by several electron-transfer dyes (52). Catalytic quantities of MB and PMS, when irradiated by visible light, have regenerated $NAD(P)^+$, respectively, in oxidations of ethanol and 6PG, respectively (53). The total turnover number reached 1125.

Regioselectivity is not the problem in the regeneration of $NAD(P)^+$ that is of the regeneration of NAD(P)H, but chemical and electrochemical strategies are not suitable here. The criterion of high total turnover number and turnover rate eliminates most chemical, photochemical and electrochemical methods of regeneration from serious considerations. The enzymatic method of cofactor regeneration is better than chemical or electrochemical methods and they are more compatible with biochemical systems.

2.6.3 Biological method with enzymes

Several enzymes have been studied for the regeneration of NADH towards NAD^+: glutamate dehydrogenase, L-lactate dehydrogenase, alcohol dehydrogenase and NADH oxidase which catalyzes the oxidations of NAD(P)H (54).

2.6.3.1 Glutamate dehydrogenase

Glutamate dehydrogenase (GluDH) catalyzes the reaction of α-ketoglutarate to glutamate and oxidizes NAD(P)H to $NAD(P)^+$. This system allows the oxidation of NAD(P)H under anaerobic conditions. A shortcoming for this enzyme is that in order to regenerate NADH towards NAD^+ it uses expensive α-ketoglutarate to generate cheap glutamate (55). Also, the formation of stoichiometric quantities of glutamate must be isolated from the final product because it will cause the inhibition of the enzyme. The specific activity of GluDH is only moderate, which is another problem of using GluDH to regenerate NAD^+. The coupled cofactor regeneration reaction cannot affect the equilibrium due to the irreversibility of α-ketoglutarate to glutamate reaction.

2.6.3.2 Lactate Dehydrogenase

Lactate dehydrogenase (LDH) is less expensive than GluDH and has a higher specific activity. It can use pyruvate and glyoxylate as its substrates. The pyruvate/LacDH system does not require oxygen and it is stable in air. LDH cannot oxidize NADPH and the system has a low reduction potential. Pyruvate is not stable in solution. It may condense with itself or decarboxylate to carbon dioxide and acetaldehyde and may add nucleophilically to NAD^+(56,57). LacDH has shown to have better turnover rates than GluDH and the system was found to be more stable than the GluDH system. Another substrate of LacDH is glyoxylate. Glyoxylate is less expensive than pyruvate.

The reduction of glyoxylate is thermodynamically more favorable than even the reductive animation of α-ketoglutarate . But glyoxylate/LacDH has a low potential. In the presence of nicotinamide cofactors, LacDH can catalyze glyoxylate to glycolate and oxalate (58). Only the small-scale reaction has been investigated.

2.6.3.3 Alcohol Dehydrogenase

Acetaldehyde, coupled with alcohol dehydrogenase (ADH), has been used to regenerate NAD^+ from NADH in preparations of fructose and cyclic ketones (59,60). The advantages of using acetaldehyde and ADH are as following: low cost of acetaldehyde and ADH; high specific activity of ADH; volatile acetaldehyde and ethanol. But the deactivation of enzymes by acetaldehyde or ethanol and the instability of acetaldehyde in solution (57) will cause trouble to the regeneration system—acetaldehyde could be oxidized to acetate. When using ADH from *L. mesenteroides* or *Thermoanaerobium brockii* (61,62), $NADP^+$ could be regenerated. During operation, the concentration of acetaldehyde should always be kept low to avoid enzyme deactivation by carbonyl addition to amino group.

2.6.3.4 NADH oxidase

Even though a large number of enzymes are known to depend on nicotinamide coenzymes, it is still necessary to screen for novel catalysts with potential technical applications. The growing importance of chiral compounds demands the use of novel enzymes with new substrate specificities (63). NADH oxidase is a better choice comparing with other cofactor-regenerating-oxidoreductases: i) the regeneration reaction helps to drive the equilibrium of the combined production-regeneration system, ii) NADH uses oxygen as its substrate, so there is no need to add substrates, iii) it does not

generate by-products and the final product water does not inhibit the enzymes involved, iv) easy separation of the product from the solution compared to GluDH and LacDH. There are two categories of NADH oxidases: hydrogen peroxide-forming NADH oxidase (nox-1, molecular oxygen reduced to hydrogen peroxide in a two-electron reduction) and water-forming NADH oxidase (nox-2, molecular oxygen reduced to water in a four-electron reduction) (64,65). In our group, a novel water-forming NADH oxidase from *Lactobacillus sanfranciscensis* (*L.san*-Nox2) has already been characterized (54,66).

The examples of using an NADH oxidase in NAD^+ regeneration have recently been demonstrated both by our group and Werner Hummel's group in Juelich/Germany. Our group employed NADH oxidase from *Lactobacillus sanfranciscensis* and (R)-alcohol dehydrogenase from *Lactobacillus brevis* to perform enantioselective oxidation of racemic phenylethanol to acetophenone and (S)-phenylethanol with regeneration of either NADH or NADPH to their respective oxidized precursors (54). Our group also used the coupled reaction with L-Glutamate Dehydrogenase and NADH oxidase from *L. sanfranciscensis* for the oxidation of mono-sodium glutamate (Figure 2.3) (55). NADH oxidase was applied in both cases for the regeneration of $NAD(P)^+$. All of these reactions took place in a laboratory scale and have not been operated in a large scale. Hummel's group used NADH oxidase from *Lactobacillus brevis* and ADH from *L. brevis to* isolate the enantiomerically pure S-isomer from racemic 1-phenylethanol (67).

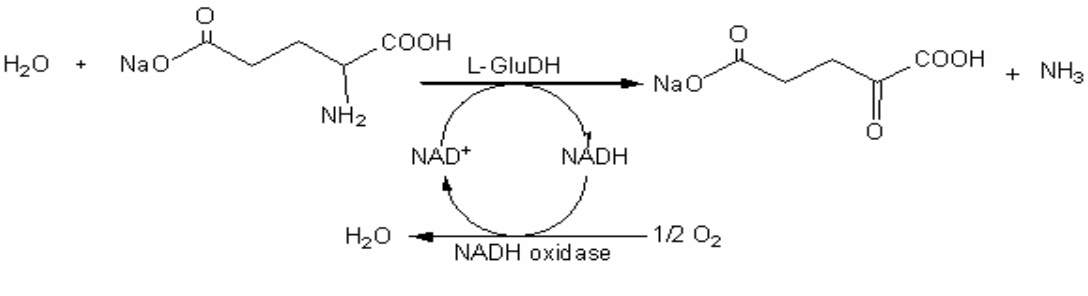

Figure 2.3: Cofactor regeneration system with L-GluDH and NADH oxidase.

My thesis will focus on finding novel NADH oxidases and applying it in the cofactor regeneration system together with carbonyl reductase from *L. lactis* (LL-CR) and horse liver alcohol dehydrogenase (HL-ADH). An example is shown in Figure: ADH takes NAD^+ as its substrate and generates NADH as its product. The coupled reaction of water-forming NADH oxidase takes NADH as its substrate and regenerate NAD^+ from NADH, which drives the equilibrium towards the product formation direction. Two methods will be investigated: whole-cell catalyst and enzyme membrane reactor with isolated enzymes, while using NADH oxidase to regenerate $NAD(P)^+$ together with HLADH/carbonyl reductase (Figure 2.4).

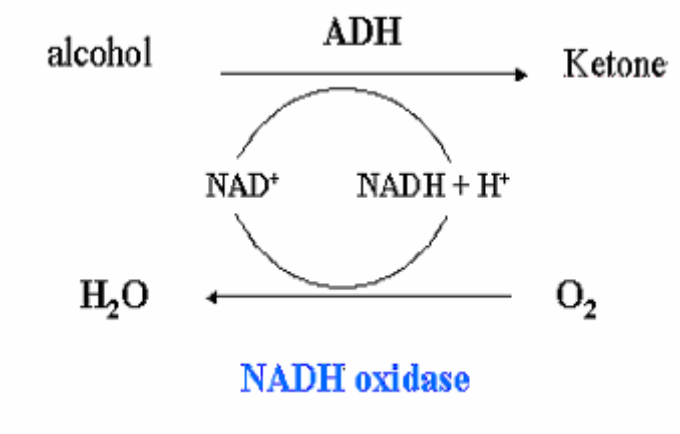

Figure 2.4 *In situ* cofactor regeneration scheme using biological method.

CHAPTER 3

ALKYL HYDROPEROXIDE REDUCTASE FROM *LACTOCOCCUS LACTIS*

3.1 Introduction

Bacteria have their own defense system against peroxide generated during metabolism. Alkyl hydroperoxide reductase is a category of non-heme, non-selenium proteins, distinct from catalases and glutathione peroxidases, which catalyze the reduction of organic hydroperoxides and hydrogen peroxide . Many members of the lactic acid bacteria family are found not to have catalase or functional electron-transfer chain and usually contains the alkyl hydroperoxide reductase gene in their genome (68). *Lactococcus lactis* (*L. lactis*), as a member of the lactic acid family, was annotated to have the alkyl hydroperoxide reductase (AhpR) gene for the defense against peroxide. In this chapter, we investigate the reduction of oxygen to hydrogen peroxide and the reduction of hydrogen peroxide to water with the help of alkyl hydroperoxide reductase from *L. lactis*.

Alkyl hydroperoxide reductase system is made up of two enzymes: nox-1 (gene name AhpF) and peroxidase (gene name AhpC). AhpF and AhpC were originally identified by Ames (69) as part of the peroxide-responsive global regulon of the OxyR transcription factor in *Salmonella typhimurium*. AhpC, the peroxide-reducing protein of the system, is a representative of a very large family of cysteine-based peroxidases, now designated as “peroxiredoxins” (Prxs). AhpF, on the other hand, is a flavoprotein expressed only by bacteria and appears to act as a dedicated “AhpC reductase” in those

bacteria (70,71). The full sequence of AhpC is just upstream of AhpF. In many AhpF-deficient organisms, the NAD(P)H-dependent recycling of AhpC or other Prxs is mediated by at least two proteins, either the thioredoxin reductase (TrxR) or the thioredoxin (Trx) system (68). Reactions catalyzed by AhpR are as follows:

nox-1: $O_2 + NADH + H^+ \longrightarrow NAD^+ + H_2O_2$ (1)

peroxidase: $H_2O_2 + NADH + H^+ \longrightarrow NAD^+ + 2H_2O$ (2)

Overall reaction:

$O_2 + 2\ NADH + 2\ H^+ \longrightarrow 2\ NAD^+ + 2\ H_2O$ (3)

Thus, the overall AhpR reaction is exactly the same as for the nox-2 enzymes (54,66).

Streptococcus mutans (*S. mutans*), *Amphibacillus xylanus* (*A. xylanus*) and *Salmonella typhymurium* (*S. typhymurium*) feature AhpC and AhpF genes as well and each has been demonstrated to produce a functional alkyl hydroperoxide reductase (72) (73) (74). There are annotated AhpF and AhpC genes from the *L. lactis* genome. Sequence alignment between nox-1 from *L. lactis* and other organisms shows identity as high as 34.1% and strong similarity up to 55.8% at the amino acid level (Figure 3.1). There is one catalytic center (CXXC) each near the N- and C-terminus, respectively.

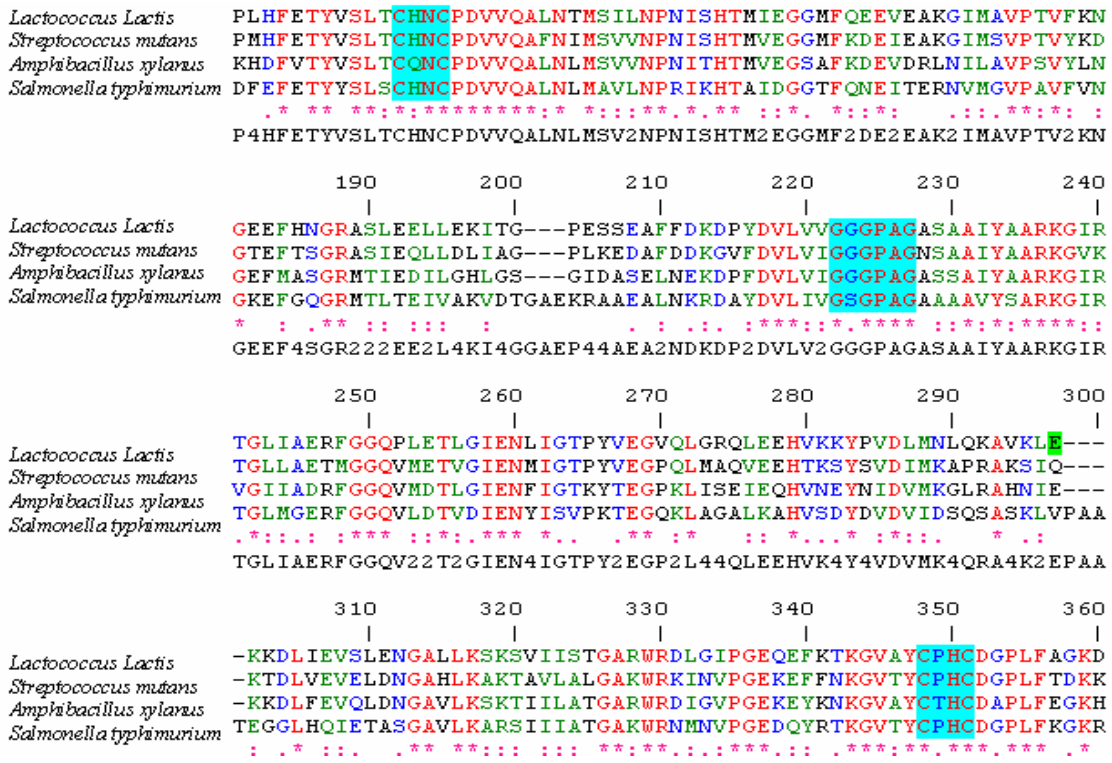

Figure 3.1: *L. lactis* nox-1 amino acid alignment with other known nox-1 proteins. Identity: 34.1%; strong similarity: 55.8%. CxxC: Catalytic Center; GxGxxG: flavin and NAD(P)H binding site

Peroxidases (AhpCs) share strong sequence similarities: sequence alignment between proteins from *L. lactis*, *Salmonella typhimurium* (*S. typhimurium*) (75), and *Amphibacillus xylanus* (*A. xylanus*) reveals identity at the amino acid level of 52% and additional strong similarity of 20% (Figure 3.2) (76).

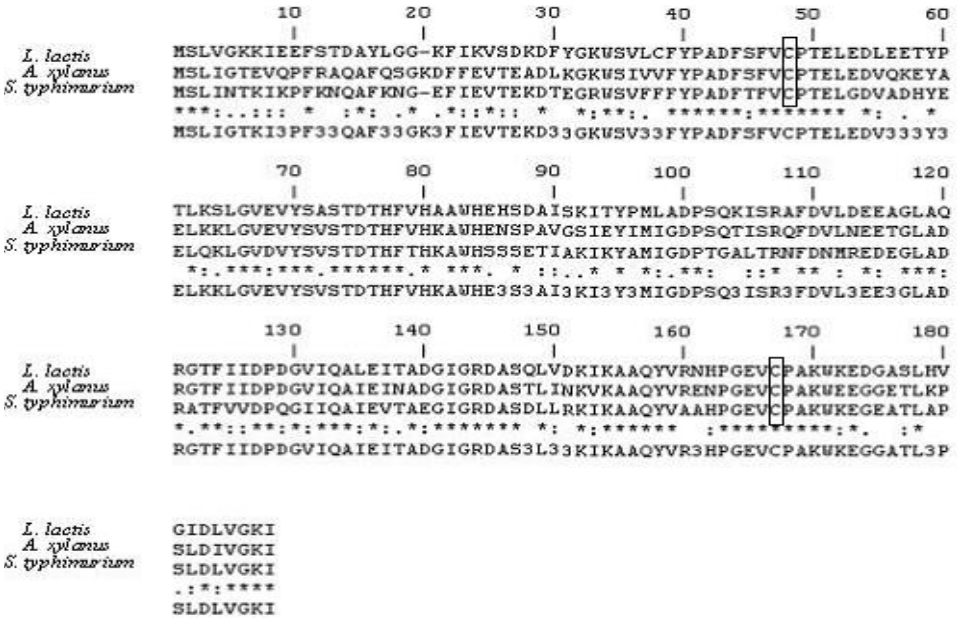

Figure 3.2: *L. lactis* peroxidase amino acid alignment with other known AhpC proteins: the highlighted C46 and C165 are catalytic Cys residues of AhpC (*L.lactis*)

The 3D structures of AhpF and AhpC from *Salmonella typhymurium* have been determined (PDB 1HYU and 1YEP, respectively) (77,78). The C-terminal 320 residues of AhpF are homologous with TrxR (35% identity) and contain the CXXCD motif required in TrxR for the dithiol-disulfide interchange reaction with Trx (corresponding to C345 and C348 in AhpF). Furthermore, AhpF possesses an additional 200 residues at the N-terminus not present in TrxR and the existence of another CxxC in this domain (C129 and C132) suggesting an additional catalytic disulfide redox center (69,74). AhpF was found to be a homodimer with each subunit being comprised of three domains (the amino acid positions are positions in *Salmonella typhymurium*): N-terminal redox-active disulfide-containing domain (NTD, 1-196), FAD binding domain (210-327, 450-521) and an NADH binding redox-active disulfide-containing domain (NADH/SS, 328-449). The

NTD is directly responsible for the ability of AhpF to reduce redox-active disulfides in AhpC (74,79).

AhpC was found to be a 210 kDa homodecamer in solution (80). 3D structure of AhpC from *S. typhymurium* shows that AhpC can only be active as a dimer—C46 from chain A and C165 from chain B form the active center C46-C165 disulfide bond (Figure 3.3). This is strong evidence that AhpC could only be active as a dimer. Electrons from the N-terminal disulfide center of nox-1 are presumed to transfer to the inter-subunit disulfide bond when AhpF and AhpC temporarily interact.

According to the amino acid alignment, both AhpF and AhpC from *L. lactis* showed strong identity and similarity with the AhpF and AhpC from *S. typhymurium*, so it is very likely that AhpC from *L. lactis* has a very similar structure as AhpC from S. *typhymurium*.

The mechanism of alkyl hydroperoxide reductase from *S. mutans* and *S. typhimurium* was proposed by Leslie Poole (Figure 3.4): demonstrating the importance of the disulfide units close to the termini for electron transport (72) (79).

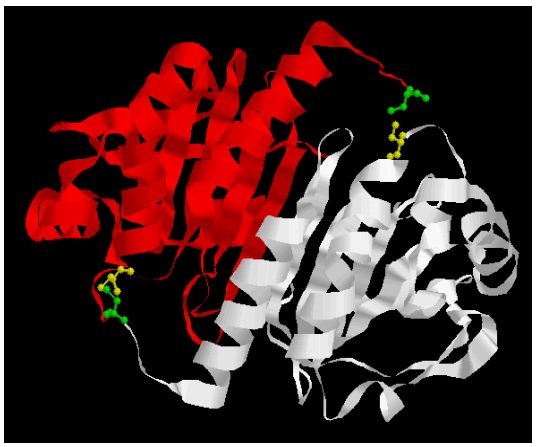

Figure 3.3: 3D structure of AhpC: the interaction between two subunits. chain A is in white and chain B is in red C46s are highlighted in green and C165s are highlighted in yellow.

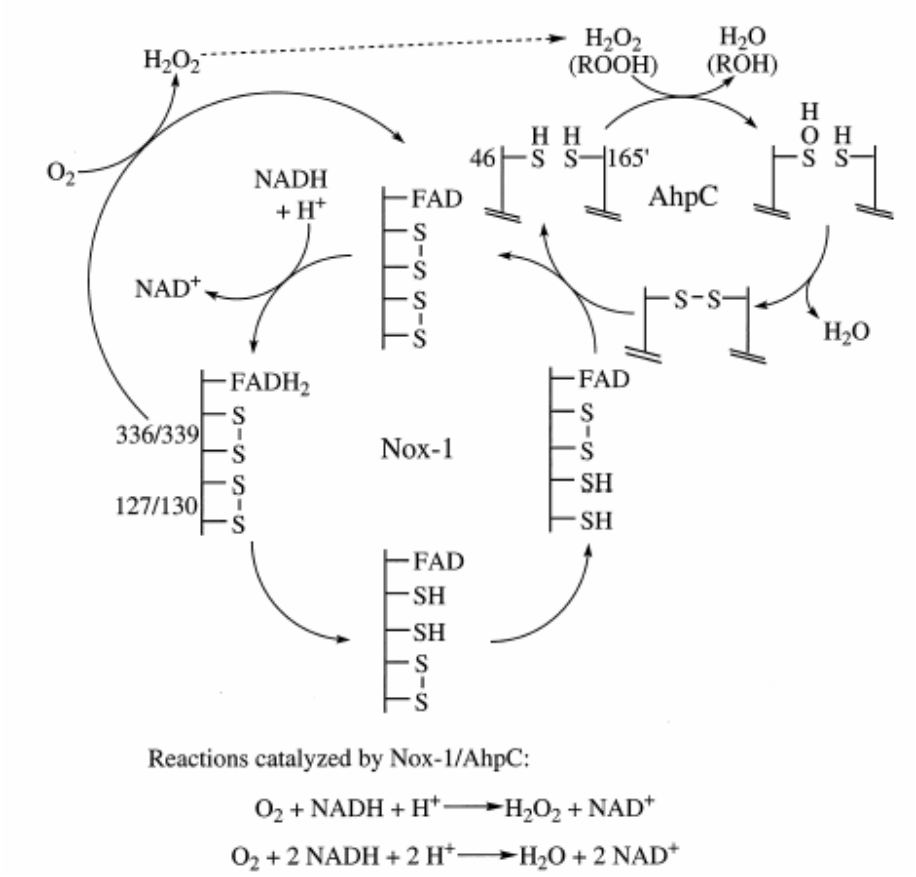

Figure 3.4: Proposed mechanism of alkyl hydroperoxide reductase from *S. mutans* (72).

Electrons transferring from NADH to FAD are followed by a conformational change, flavin reduces the C-terminal disulfide bond (C336/339), and the C-terminal disulfide then transfers its electrons to the N-terminal disulfide bond (C127/130) and reduces it to its dithiol form. This is due to the N-terminal disulfide bond at the interface of AhpF and peroxidase that makes it easier to transfer its electrons to the peroxidase disulfide bond. The electrons finally are transferred to the hydrogen peroxide produced from AhpF reaction and forms water. AhpC is inactive in the absence of Nox-1, while

Nox-1 is active in the absence of AhpC. Table 3 shows the Nox-1 and AhpC catalytic activities from different microorganisms. Since the Nox-1 activity is lower than 10U/mg, it is necessary to obtain more active Nox-1 from other sources.

Table 3.1: Comparison of Catalytic Activities of alkyl hydroperoxide reductase

	S. mutans		*S. typhimurium*	
	AhpF	AhpC	AhpF	AhpC
Oxidase(U/mg)	9.8*	ND	1.96	ND
Peroxide reductase activity(H_2O_2)	9960[b]		1530[a]	460[a]

*Enzyme was purified directly from the lysate of *S. mutans* and has S.A. 37U/mg (81)
[a]AhpF activities were expressed as unit per micromole of FAD, and AhpF were assayed in the presence of 5nmol of recombinant AhpC. AhpC, samples were assayed in the presence of 5nmol of recombinant AhpF (72)
[b]Values were give as Unit per micromole bound FAD, assays performed anaerobically with [AhpC] varied from 3 to 50uM in the presence of 0.5uM flavoprotein (72).

Peroxiredoxins are a family of thiol-specific antioxidant proteins, also termed the thio-redoxin peroxidases and alkyl-hydroperoxide-reductase proteins (AhpC). Prxs exert their protective antioxidant role in cells through their peroxidase activity, whereby hydrogen peroxide, peroxynitrite and a wide range of organic hydroperoxides (ROOH) are reduced and detoxified (74,80). These enzymes have been found in yeast, plant and animal cells and eubacteria and archaea. AhpC, as a member of this peroxiredoxin family, has the typical 2-Cys active sites. The structure and the sequence of AhpC are very similar to the other Prxs such as the human peroxidase (82,83).

Previous work with the peroxidase AhpC showed that it is not an independent enzyme, i.e., its activity is coupled to interaction with AhpF-like enzymes. Leslie Poole's group demonstrated AhpC's activity by the anaerobic AhpF-dependent peroxidase assay (5nmol AhpC, 10-75 pmol AhpF) and AhpC-dependent peroxidase assay (5 nmol AhpF and 100-200 pmol AhpC) (72). Here, we monitor production of hydrogen peroxide to verify the activity of our AhpC from *L. lactis* with different AhpF/AhpC ratios and characterized its stability together with AhpF for the biocatalytic process.

3.2 Materials and Methods

3.2.1 Cloning and overexpression

The AhpF and AhpC genes from *Lactococcus lactis* were isolated from the genomic DNA using gene specific primers derived from the coding sequence. AhpF and AhpC were successfully amplified by the polymerase chain reaction (PCR) using the Failsafe Kit (Epicenter, Madison, WI). The primers for PCR were 5' AATGTCATTAGTAGG TAAAAAAATAGAAG 3' (AhpC forward primer) and 5' TCTATATTTTACCTACAAGGTCAATACC3' (AhpC reverse primer); ATG ATTTTAGATGAAACTCTTC (AhpF forward primer) and TTAGTTTCTTATTAAATAATCA (AhpF reverse primer). AhpF and AhpC PCR product was then purified through gel electrophoresis and subsequent elution (Gel Extraction Kit, Qiagen, Valencia, CA). Both were then cloned into pDrive vector that encoded blue/white screening feature (Qiagen PCR Cloning kit, Qiagen, Valencia, CA), and transformed into Qiagen EZ competent cells. Positive clones were identified as white colonies. The recombinant pDnox1 and pDahpC was obtained through miniprep (Qiagen Spin Miniprep kit, Qiagen, Valencia, CA), analyzed by PCR and sequenced.

The pDnox1 and pDahpC construct were used as template for the PCR of the desired gene AhpF and AhpC. The PCR products were subcloned into the expression vectors pET32 and pET30, respectively (EK/LIC cloning kit, Novagen, Madison, WI). Primers were designed as required: GACGACGACAAGATGATTTTAGATGAAACTCTTC and GAGGAGAAGCCCGGTTTAGTTTCTTATTAAATAATCA. The pET32 vector has a thioredoxin tag, a His tag, and an S tag (for increase of protein solubility) on its N-terminus. The pET30 vector has a 6xHistidine tag and an S tag on its N-terminus.

Subcloning was successful and the recombinant was first transformed into NovaBlue cells for positive/negative test and then recombinants pET32nox1, pET30nox1 and pET30ahpC were transformed into the chemically competitive strain BL21(DE3)-RIL (Stratagene, La Jolla, CA).

The successful clones pET32nox1, pET30nox1 and pET30ahpC were grown in LB broth with 50μg/mL ampicillin and 50μg/mL chloramphenical at 30^{o}C for 4h. The protein expression was induced with 167 μM isopropyl β-D-thiogalactopyranoside (IPTG) at an OD_{600} of 0.5~0.6, overexpression conducted at 20^{o}C, and protein harvested after 2.5 h. At 20^{o}C, pET32nox1 expressed a higher amount of soluble protein than at 30 and 37^{o}C. The pellet from a 400 mL culture was then suspended in 15 mL 50mM sodium phosphate buffer at pH 7 containing 300 mM NaCl and destroyed by sonication (8 x 30sec, 1min pause).

3.2.2 Purification and Dialysis of nox-1

By taking advantage of the N-terminal 6xHis tag on nox-1, the protein was purified by using Immobilized Metal Affinity Chromatography (IMAC; BD TALON Co2+ Metal Affinity CellTru Resin, BD Biosciences, Palo Alto, CA). The soluble fraction of the destroyed cells was loaded to the Co^{2+} resin column previously equilibrated with pH 8 50mM sodium phosphate buffer with 300 mM NaCl. After the binding step, the resin was washed four times with pH7 50mM sodium phosphate containing 300 mM NaCl and 15 mM imidazole. With pH 7 PPB buffer 150mM imidazole, the protein was eluted from the column. The protein was then dialyzed overnight against pH7 50mM HEPES, 1mM EDTA buffer, using a UF membrane with 12~14 kDa MWCO (Spectrum Laboratories, Rancho Dominguez, CA); buffer was

changed twice. Protein concentration was measured by the Bradford assay after 5min incubation with Coomassie Protein Assay Reagent (Pierce, Rockford, IL) using the Biophotometer (Eppendorf, Westbury, NY).

Dialysis during reconstitution experiments of apo-enzyme nox-1 with FAD was conducted at pH 7.0, in 50mM HEPES buffer, with 1mM EDTA and either 0 or 2 M NaBr added.

3.2.3 Wavelength-scan of nox-1 holoenzyme

After purification, nox-1 is colorless owing to its presence as an apo-enzyme. To reconstitute the holoenzyme, 9.1 μM nox-1 apo-enzyme were incubated with a 30-fold molar excess of FAD at 30^{o}C for 10 min. Excess FAD was removed from the protein solution by gel permeation chromatography over a PD-10 column (Amersham, Sweden). The eluent fraction with the highest volumetric activity was scanned from 250 nm to 700 nm in a quartz cuvette.

3.2.4 Amplex Red assay for H_2O_2

We employed the horseradish peroxidase (HRP)-catalyzed oxidation of 9-acetylresorufin ("Amplex Red", Molecular Probes, Eugene, OR) to fluorescent resorufin as our H_2O_2 assay. Amplex Red (Figure 3.5) reacts with H_2O_2 according to a strict 1:1 stoichiometry, large extinction coefficient (ε: 54,000 L/(mol·cm), λ_{max}: 587 nm (emission)), and an extremely low detection limit of 100 nM resorufin product. A 10 μL sample was pipetted into a 96-well microplate after the reaction with 800 μM NADH was completed. Working solution including HRP and Amplex Red was subsequently added, the reaction was finished after 30 min in the dark. A Fluorostar (BMG Labtechnologies, Durham, NC) platereader was used to detect resorufin fluorescence. Seventy five units of

superoxide dismutase from bovine erythrocytes (Sigma-Aldrich, Milwaukee, WI) was employed to test for formation of superoxide ion during the nox-1 reaction. Samples from the reaction were tested for H_2O_2 with Amplex Red as well. Samples from the reactions of nox-1, alkyl hydroperoxide reductase (AhpF/AhpC 1:1, 1:20, 1:200) were pipetted into a 96-well microplate after the reaction with 0. 1 mM NADH.

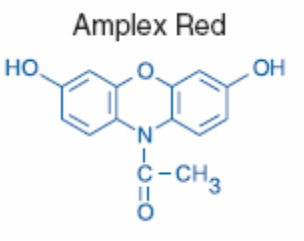

Figure 3.5: Amplex Red structure

3.2.5 Nox-1 kinetics

A DU-800 spectrophotometer (Beckman Coulter, CA) was used to detect nox-1 activity by following the decrease of substrate NADH absorbance at 340nm (ε: 6220 $M^{-1}cm^{-1}$). Both disposable 1.75 mL UV transparent cuvettes (light path 1cm, VWR, NJ) and 1.7 mL quartz cuvettes (light path 5mm) were used. The measurement of kinetic parameters with substrate NADH and cofactor FAD was performed with nox-1 in air-saturated pH 7 50mM HEPES solution at 30°C. Nox-1 was first incubated with FAD of a given concentration at 30°C for 5-7 min before adding NADH.

The K_D value of the cofactor FAD is determined at varying FAD concentration from 3.33 to 500 μM. Standard conditions were then set at 30°C, 53 μM FAD, incubation of nox-1 for 5-7 min, 0.24 mM NADH, pH 7 50mM HEPES buffer. The K_M value of

NADH is determined by 0.01-0.48 mM NADH at an FAD concentration of 53 μM (= K_M of FAD).

Inhibition by NAD^+ was investigated at [NAD^+] of 0, 0.24, 0.48, and 0.72mM at different NADH concentrations. Product inhibition by H_2O_2 was investigated by adding 0, 5.87, 11.73, or 17.61mM of H_2O_2. K_I can be calculated from the intercepts on the Lineweaver-Burk plot: $K_I = [I]/(v_{max} * \text{intercept} - 1)$.

Catalase (0.4-7.2U) from *Aspergillus niger* (SAF, Milwaukee, WI) was added to 4.5 μM nox-1 and NADH solution to check for any improvement in activity.

3.2.6 Measuring total turnover number

A specific amount of nox-1 was added to the 1.5 mL air-saturated 50mM HEPES buffer +/- 5mM DTT at pH 7.0, 30°C. NADH was added until the enzymes could no longer react.

3.3 Results

3.3.1 DNA sequencing of AhpF

DNA sequencing data of pET32nox1 shows that it has five silent "mutations" and the E290R mutation (GAG to AGG), compared to the annotated gene sequence in the NCBI database (1560bp). The reason is probably that the NCBI *L .lactis* strain is different from what we have bought from ATCC. PCR product of the AhpF gene is shown in Figure 3.6.

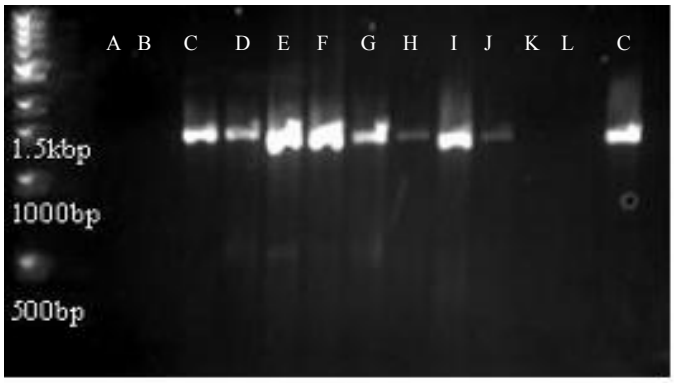

Figure 3.6: PCR of AhpF using Failsafe kit (Buffer A-L). Buffer E and F are the best buffer for AhpF. PCR product is 1560bp.

3.3.2 DNA sequencing of AhpC

DNA sequencing data of AhpC PCR product (Figure 3.7) and pET30ahpC revealed one silent mutation (TCG to TCA) at Ser63, compared to the annotated gene sequence in the NCBI database (564bp).

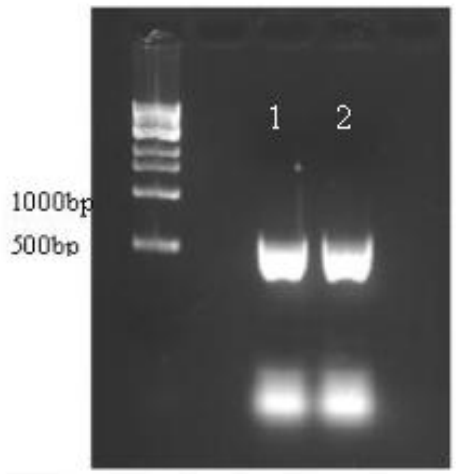

Figure 3.7: PCR product of AhpC. Lane 1 and lane 2 show AhpC PCR products on the gel and the size is around 564 bp.

3.3.3 Purity and yield

Nox-1 was overexpressed to 6.45% of cell soluble protein at a level of 25.8 mg/L under the conditions mentioned above. After purification over IMAC, the overall activity yield was 35% (at a protein concentration of 0.6 g/L). Results of electrophoresis (12% SDS-PAGE) of lysate and purified protein are featured in Figure 3.8, the protein was judged to be >95% pure.

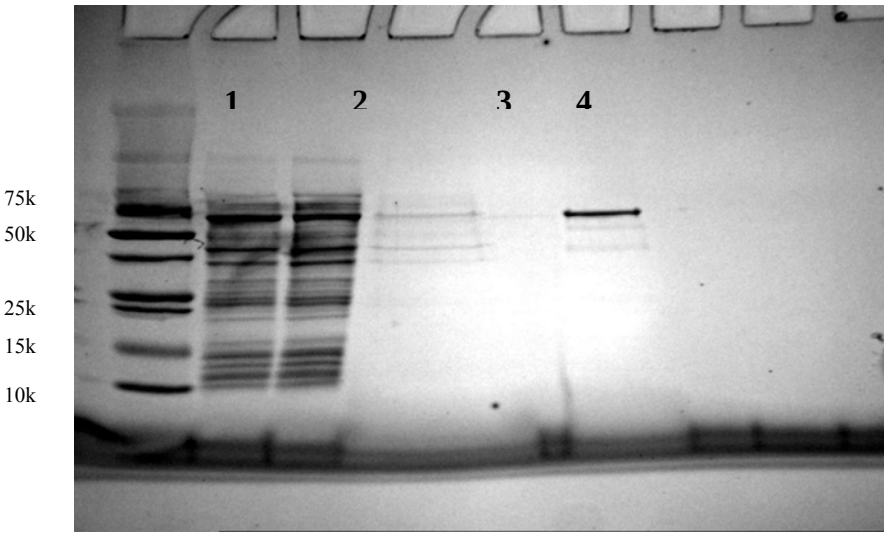

Figure 3.8: Purification of nox-1. 12% Tris Glycine SDS-PAGE gel. Lane1 and 2: lysate; Lane 3: run-off after 1st wash; Lane 4: run-off after 2nd wash; Lane 5: protein purified (~ 67kDa). Nox-1 is around 55kDa and N-terminal tags are 12kDa.

The open reading frame for AhpC is capable of encoding a protein with a molecular mass of 22kDa, which is in good agreement with previously published similar alkyl hydroperoxide peroxidases. SDS-PAGE of the proteins derived from the expressed genes exhibited prominent bands at the right size (Figures 3.9).

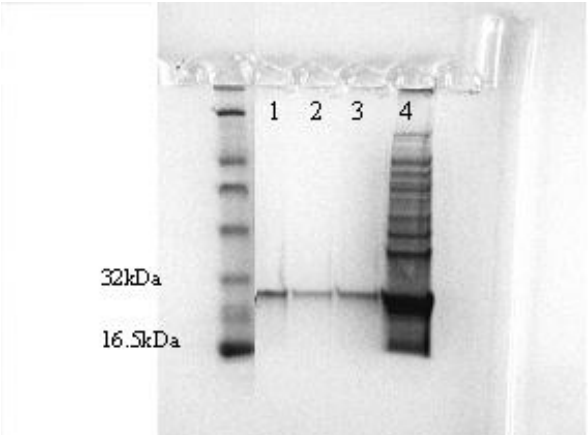

Figure 3.9: Purification of AhpC. 12% Tris Glycine SDS-PAGE gel. Lane 1-3: protein purified (~21kDa); Lane 4: lysate

3.3.4 Reconstitution of nox-1 apo-protein with FAD

The nox-1-containing solution eluting off the Co^{2+}-resin column was colorless, consistent with the presence of apo- protein. To reconstruct nox-1 holo-enzyme, we proceeded to incubate the apo-protein with different amounts of FAD while varying temperature (4 vs. 30°C), incubation time (5 min vs. overnight), and dialysis in the absence vs. presence of 2 M NaBr to render its conformation more flexible, thus possibly easing FAD incorporation into the apo-protein (84).

Incubation temperature turned out to be the crucial factor: incubation of apo-protein nox-1 with FAD at 30°C for 5 min yielded the highest level of activity, considerably higher than incubation at 4°C. The lower level of activity after overnight incubation at 30°C, might be attributed to the onset of degradation of the apo-protein. Dialysis in the presence of 2M NaBr did not yield any improvement in activity.

3.3.5 FAD/subunit

From the scan of the nox-1 holo-enzyme (Figure 3.10), we found an absorbance ratio A_{450}/A_{280} of 0.108, a ratio characteristic of a pure flavoprotein with one FAD molecule per subunit of nox-1. The absorbance peaks at 378nm and 445nm corroborate nox-1 to be a flavoprotein with flavin in its oxidized form (the solution was air-saturated). Nox-1 holoenzyme was found to feature a specific activity of 2.04 U/(mg protein) at 0.24 mM NADH, 30°C, and pH 7.

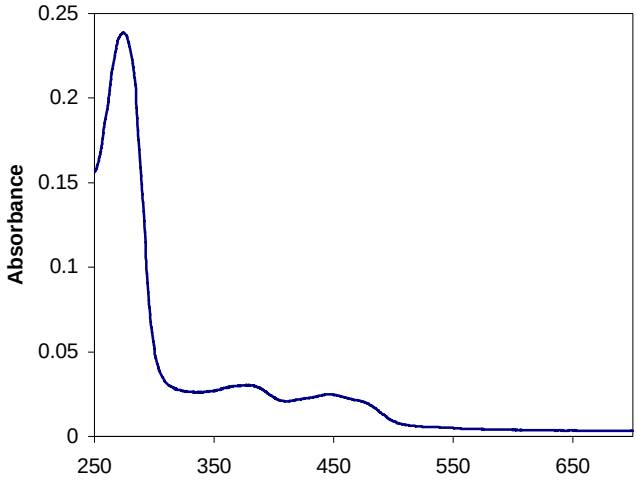

Figure 3.10: UV visible absorbance spectrum of reconstituted holo-hydrogen peroxide forming NADH oxidase. Nox-1 was first incubated with 30-fold FAD before PD-10 column treatment. 50mM HEPES, 1mM EDTA, pH 7, 30ºC. Absorbance peaks: 378nm and 445nm .

3.3.6 Kinetic parameters of nox-1

The K_D value of the cofactor FAD was found to be 54 μM, measured in the presence of 0.24 mM NADH; the apparent maximum velocity $v_{max,app}$ ($[O_2]$ = 0.25 mM = const. in the air-saturated solution, [NADH] = 0.24 mM) was 0.98 μmol/(L·s), resulting in an apparent maximum specific activity of 14.6 U/mg, as evidenced by the Hanes plot (Figure 3.11). The K_M value of NADH, measured at 53 μM FAD, which is close the Kd value of FAD, was found to be 76 μM, resulting in a maximum specific activity of 30 U/mg (Figure 3.12). After adding catalase, no increase in nox-1 activity was observed.

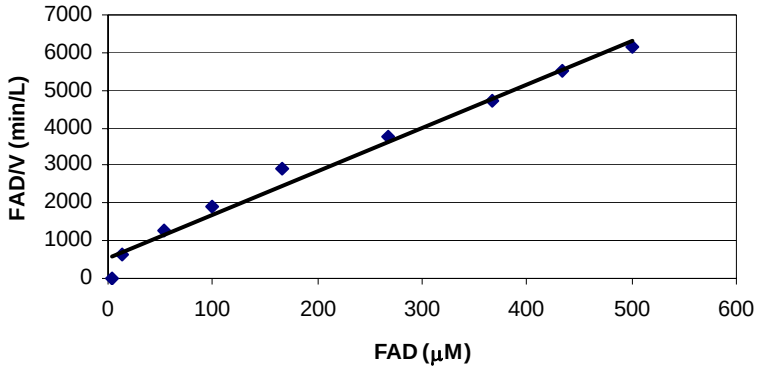

Figure 3.11: Kinetics of nox-1 with cofactor FAD. Air-saturated, pH7, 50mM HEPES, 0.24mM NADH, 30ºC. Hanes plot: K_M of FAD is 53µM and maximum specific activity is 14.6U/mg. K_M = 76 µM

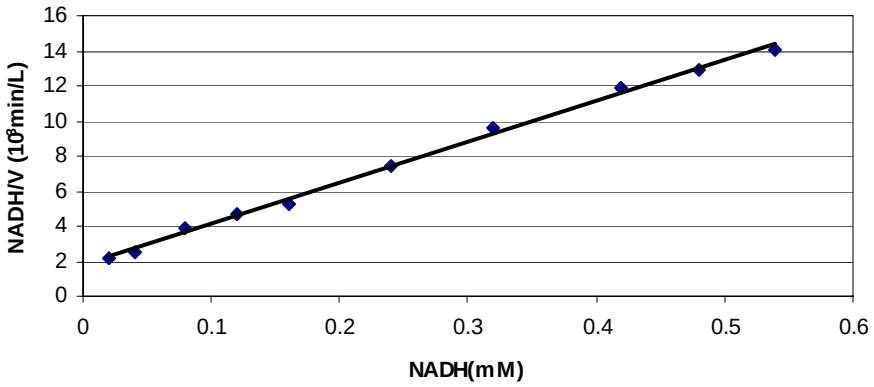

Figure 3.12: Kinetics of nox-1 with substrate NADH. pH7 50mM HEPES, 53µM FAD, 30ºC. Hanes Plot. K_M: 76µM, S.A. max: 30 U/mg.

3.3.7 Product Inhibition

We found that both products NAD^+ and hydrogen peroxide inhibit nox-1. Hydrogen peroxide inhibits the enzyme non-competitively (Figure 3.13), with an inhibition constant K_I about 12 mM. This constant is comparatively large: even at 17.6 mM, our highest H_2O_2 concentration investigated, the enzyme is still rather active. On

the other hand, NAD^+ is a strong inhibitor. While we could not establish a definite inhibition constant due to scatter, we estimate the K_I to be in the range of 0.2 mM.

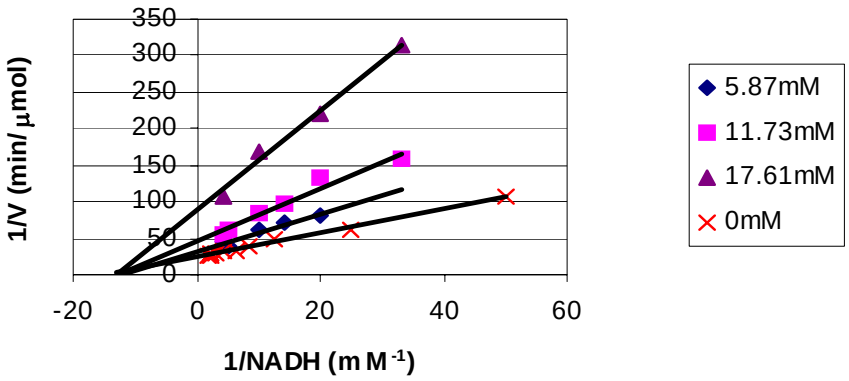

Figure 3.13: Noncompetitive inhibition from H_2O_2. Lineweaver-burke plot. K_I is around 12mM.

3.3.8 Total turnover number (TTN)

The total turnover number (TTN) (total product produced/amount of enzyme [mol/mol]) of nox-1 during our experiments at 30 ºC and pH 7 was found to be 44,000 based on conversion of NADH. This result indicates good stability of our enzyme against turnover-based inactivation. The total turnover number of AhpF is not affected by the amount of added AhpC. The TTNs are not affected by the addition of the DTT, which is not the case in the water-forming NADH oxidase.

Table 3.2: Total turnover number of AhpF and alkyl hydroperoxide reductase

TTN	AhpF/AhpC (1000:1)	AhpF/AhpC (1:1)	AhpF/AhpC (1:20)	AhpF
HEPES	82,000	82,000	82,000	82,000
HEPES, 5mM DTT	82,000	82,000	82,000	82,000

3.3.9 Coupled reactions with catalase and superoxide dismutase

As H_2O_2 inhibits and possibly also even deactivates nox-1, we coupled nox-1 with an excess of catalase to investigate the influence on the rate of nox-1, as measured by NADH consumption. As expected, we did not find any H_2O_2 when checking with Amplex Red after joint incubation of nox-1 and catalase, indicting that catalase indeed converted all generated H_2O_2 to O_2 and water. This finding also demonstrates the stability of nox-1 against stoichiometric levels of H_2O_2 formed when converting NADH.

3.3.10 Hydrogen peroxide formation of Nox-1 and AhpR

To check stoichiometry of NADH consumption and H_2O_2 generation according to equation (1), we measured H_2O_2 generation by detecting resorufin with the Amplex Red assay (see Section 2.4). We consistently detected 40 μM resorufin, equivalent to formation of 40 μM H_2O_2, upon conversion of 80 μM NADH with nox-1 holo-enzyme. Thus, we found only half of the electrons from NADH transferred to H_2O_2 (in theory, 80μM H_2O_2 should be formed). We surmised that the other half might have been reacted to superoxide in a one-electron reduction; consequently, we added superoxide dismutase (SOD) to aerated solutions of nox-1 and NADH. SOD would cause any present

superoxide to dismutate to O_2 and H_2O_2, so the level of resorufin measured in the Amplex Red assay would have to be increased, reflecting the action of SOD. However, we did not find any increase in the level of H_2O_2 produced, so superoxide is not formed in significant amounts. We shall keep investigating the cause of the discrepancy between NADH consumed and H_2O_2 formed.

To check H_2O_2 generation of alkyl hydroperoxide reductase and nox-2 from *L. lactis*, we measured the H_2O_2 generation by detecting resorufin with the Amplex Red assay (66). We found that, at an AhpF/AhpC-ratio of 1:1, the H_2O_2 generated is the same as the control of AhpF alone. When the AhpF/AhpC-ratio is 1:20, 30% less H_2O_2 was generated comparing with the control. Only when the AhpF/AhpC-ratio reached 1:200, no H_2O_2 was detected. Therefore, AhpC needs to be present in large excess to be an effective H_2O_2 scavenger.

3.4 Discussion and Conclusion

We have successfully applied the sequence comparison-based approach to find novel alkyl hydroperoxide reductase from *Lactococcus lactis* that converts oxygen to hydrogen peroxide and then to water. The amino acid sequence alignment of nox-1, AhpC from *L. lactis* shows high identity with nox-1 from *Streptococcus mutans*, *Salmonella. typhymurium* and *Amphibacillus xylanus*. There are discrepancies of the sequences in the database with those found experimentally in this work.

Whereas most currently accessible nox-2 enzymes feature tightly bound FAD coenzymes, nox-1 enzymes apparently bind FAD non-covalently (1,54,66,67,85). We measured an apparent maximum specific activity of *L. lactis* nox-1 of 15 U/mg, compared to 9.8 U/mg for the *S. mutans* and 1.96 U/mg for the *S. typhymurium* enzymes (72). Interestingly, our specific holo-nox-1 activity of 2.04 U/mg is very close to that number. No information, including K_M values, regarding exogenous addition of FAD is provided for the nox-1 from *S. mutans* and *S. typhymurium*. The maximum specific activity of 15 U/mg found for our enzyme is about an order of magnitude smaller than values found for nox-2 enzymes of *Lactobacillus sanfranciscensis* (221 U/mg) or of *Lactobacillus brevis* (116 U/mg) (55) (85). While our nox-1 enzyme from *L. lactis* is inhibited by both products NAD^+ and H_2O_2, both the large value of K_I for H_2O_2 as well as the results with the coupled catalase reaction suggest that nox-1 is surprisingly stable against H_2O_2. The results on total turnover for nox-1 (AhpF) indicate that the presence of AhpC at any stoichiometric ratio does not seem to enhance nox-1 operational lifetime. This points to deactivation not from hydrogen peroxide released from the nox-1 molecule but from hydrogen peroxide (or a subsequent product) generated by turnover even before

release. Exogenously added DTT has no effect on total turnover of nox-1, as expected, as the second thiol acts as a stabilizing nucleophile.

The reason for the loss of FAD could be that metal Co^{2+} hydrates FAD during the purification of nox-1. If other metals like Ni^{2+} or ion-exchange chromatography method were applied for purification, then the problem of losing FAD may be avoided.

In conclusion, we have successfully applied the sequence comparison-based approach to find a novel H_2O_2-forming NADH oxidase functionality in *Lactococcus lactis* from an annotated part of the genome. A very sensitive assay for hydrogen peroxide, based on fluorescence of resorufin rather than UV-VIS spectroscopy of ABTS, has been employed successfully to demonstrate that only half of the electrons from NADH were transferred to hydrogen peroxide in experiments with isolated nox-1. The two most important future tasks concern the fate of the other half of the electrons donated by NADH not currently found as H_2O_2 as well as the influence of the peroxidase (AhpC) found upstream on the genome of *L. lactis*.

CHAPTER 4

CHARACTERIZATION OF WATER FORMING NADH OXIDASE FROM *LACTOCOCCUS LACTIS*

4.1 Introduction

Many oxidative biological redox reactions require nicotinamide cofactors, such as the dehydrogenase-catalyzed transformation of monosodium L-glutamate (MSG) to α–ketoglutarate (55). The regeneration of the co-produced cofactor NADH to NAD^+ is essential for efficient transformation, especially on large-scale — not only for cofactor economics but also to drive the production reaction towards completion. Both kinds of NADH oxidase, nox-1 and nox-2, can catalyze the irreversible reduction of oxygen (63).

$$O_2 + 2\,NADH + 2\,H^+ \longrightarrow 2\,NAD^+ + 2\,H_2O \qquad (4.1)$$

The overall AhpR reaction is identical to the nox-2 enzyme (Equation 4.1). Several organisms, among them *Lactococccus lactis* (*L. lactis*), important in the dairy industry, possess an alkyl hydroperoxide reductase (AhpR) system as well as a nox-2 enzyme. Owing to its importance, the genome of *L. lactis* IL1403 was published in 1999 (86). The *L. lactis* genome contains several annotated nox-2 genes as well as both the AhpF and the AhpC genes. *Streptococcus mutans* (*S. mutans*), also a member of the lactic acid bacteria family, has been shown to have both hydrogen peroxide-forming

NADH oxidase (nox-1) and water-forming NADH oxidase (nox-2) (73,81). Nox-2 from *S. mutans* was reported to play an important role in regenerating NAD^+, whereas nox-1 was found to contribute only negligibly (87).

Most *Lactobacilli* and *Lactococci*, members of the lactic acid bacteria family, have no functional electron-transfer chain and do not possess any heme-containing enzymes, such as catalases. Their aerotolerance is related to their ability to induce flavin-dependent NADH oxidase (against molecular oxygen) and superoxide dismutase (against superoxide) (72). Thus, NADH oxidase is part of the oxygen defense system of facultative anaerobes such as *Lactobacilli* and *Lactococci*. Recent studies have shown that the NADH oxidases from *Archaeglobus fulgidus*, *Streptococcus pyogenes*, *Streptococcus mutans* and *Lactobacillus delbrueckii* play very important role to their aerobic metabolism under conditions of oxidative stress (88-90).

In Figure 4.1, *Streptococcus pyogenes* (wild type) showed that it can bear high concentration of oxygen when the nox gene is kept intact. On the other hand, when the nox gene of *Enterococcus faecalis* was mutated at its active site, C42 position, to Ser, there were no colonies growing on the plate when the oxygen concentration is high. This suggests that the oxidative stress is managed by NADH oxidase in lactic acid bacteria (91).

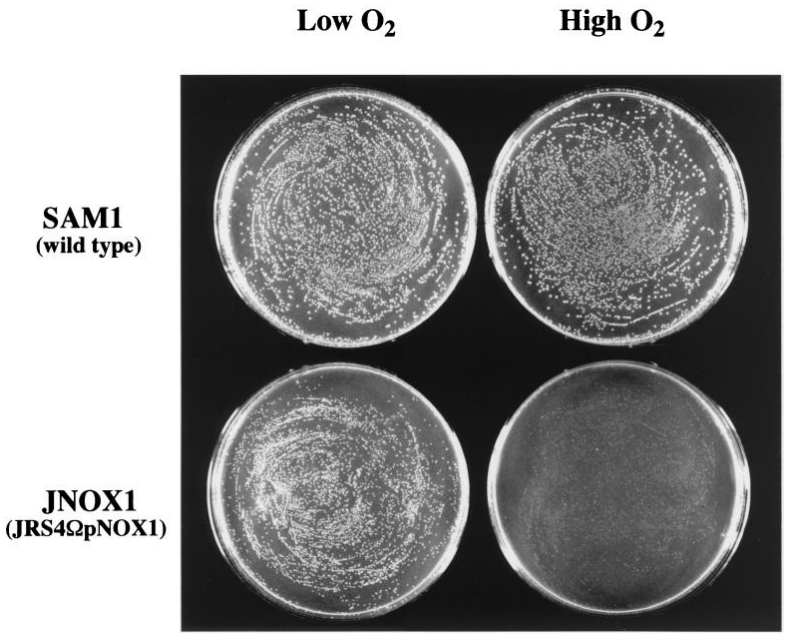

Figure 4.1: *Streptococcus pyogenes* (SAM1, wild type) and *Enterococcus faecalis* (JNOX1, nox-2 gene knocked out) shows differently under oxygen stress.

Water-forming NADH oxidase (nox-2) from *L. lactis* and its relatives, nox-2 from *Lactobacillus plantarum, Lactobacillus sanfranciscensis,* and *Streptococcus mutans* feature 20% identity at the amino acid level among themselves, and an additional strong similarity of 23% (Figure 4.2). C42 is the active center of these NADH oxidases. Alignment of the *L. lactis* nox-2 shows a conserved Cys42 active site, as in many other water- forming NADH oxidases from *Lactobacillis sanfransciscensis* (*L. sanfransciscensis*)(54,66), *Enterococcus faecalis* (92), *S. mutans* (1,81), or *Lactobacillis brevis* (67).

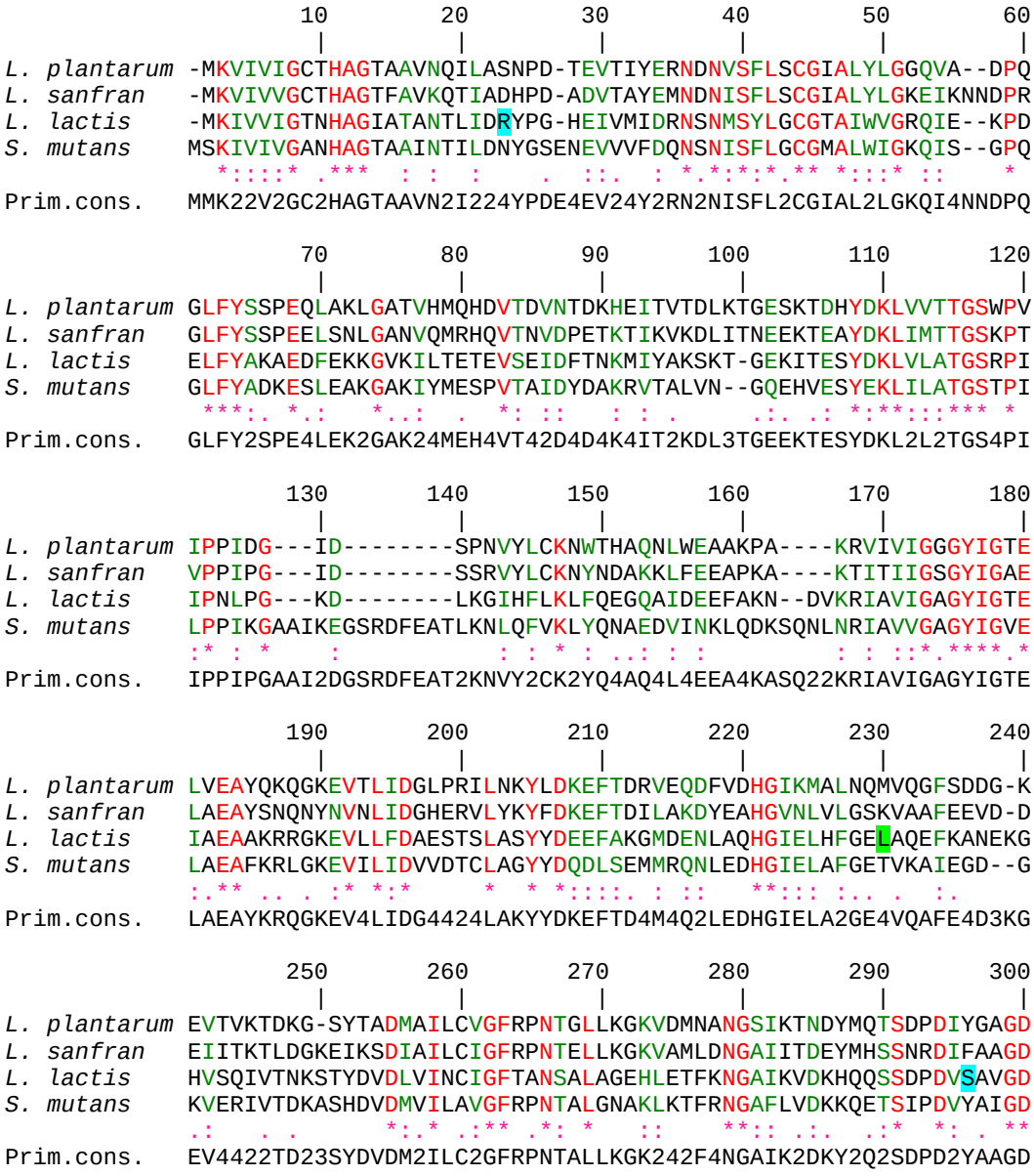

Figure 4.2: *L.lac*-Nox2 amino acid alignment with other nox-2s. All of these nox-2s have the conserved C42 at their active sites

Sequence analysis with related enzymes suggest that a redox active cysteine residue (Cys42 from both *L.san/lac*-Nox2 enzymes) alternates between the thiol/thiolate and the sulfenic acid states during turnover (93,94). The first equivalents of NAD(P)H

and O_2 yield H_2O_2, which then reacts with Cys42 to form the Cys42-SOH intermediate and a water molecule (Figure 4.3). The second equivalent of NAD(P)H is then used to reduce the sulfenic acid intermediate to the thiolate and releases the second H_2O molecule. The role of the sulfenic acid intermediate is supported by analysis of Cys→Ser mutants in homologous enzymes to create isoforms that produced H_2O_2 instead of water during turnover (95-97). Thus the *L.san/lac*-Nox2 and other homologous enzymes have evolved an efficient mechanism to protect the organism from oxidative stress. Moreover, the role of cysteine-sulfenic acids in biology and oxidative stress is quite prevalent in nature including humans (98-100).

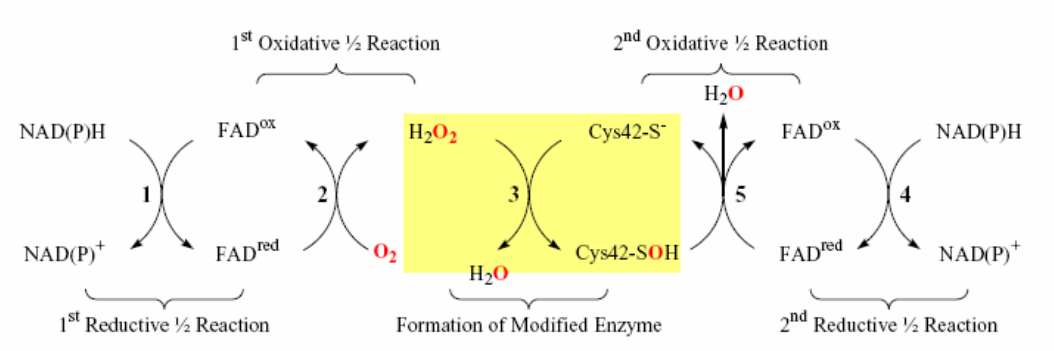

Figure 4.3: Proposed Mechanism of water-forming NADH oxidase

Another water forming NADH oxidase is from *L. sanfranciscensis* (54) has been demonstrated to use not only NADH (G37D) but also NADPH(wild type) as its substrate resulting in a very high specific activity (S. A., 220.9 U/mg). By putting the Nox-2 with the (R)-alcohol dehydrogenase (ADH) from *Lactobacillus brevis* in the reaction solution, the coupled reactions produced acetophenone and (S)-

phenylethanol with 50% yield after 12 hours(54). But the TTN of L.san-Nox2 is only around 5000 when DTT is not present.

The 3-D structure of *L.san*-Nox2 was recently established by our collaborator, Dr. Allen Orville and his coworkers. The crystal structure of *L.san*-Nox2 was obtained at 1.8 Å resolution (101) (Figure 4.4). The enzyme was found to be a dimer with each monomer consisting of a FAD binding domain (residues 1-120), a NAD(P)H binding domain (residues 150-250), and a dimerization domain (residues 325-451). The electron density for the redox-active Cys42 residue located adjacent to the *si*-face FAD is consistent with oxidation to the sulfenic acid (Cys-SOH) state. The side chain is also observed in two conformations; in one the sulfenic acid is hydrogen bonded to His10, which also adopts two conformations, and in the other it hydrogen bonds with the FAD O2' atom. The surprising finding is: the NAD(P)H binding domains each contain an ADP ligand as established by electron density maps and MALDI-TOF analysis. The ADP ligand co-purifies with the enzyme and its presence does not inhibit enzyme activity.

According to amino acid alignment, *L. lac*-Nox2 and *L. san*-Nox2 have 34% identity, so we suppose that the *L. lac*-Nox2 would also have the similar 3-D structure as *L. san*-Nox2.

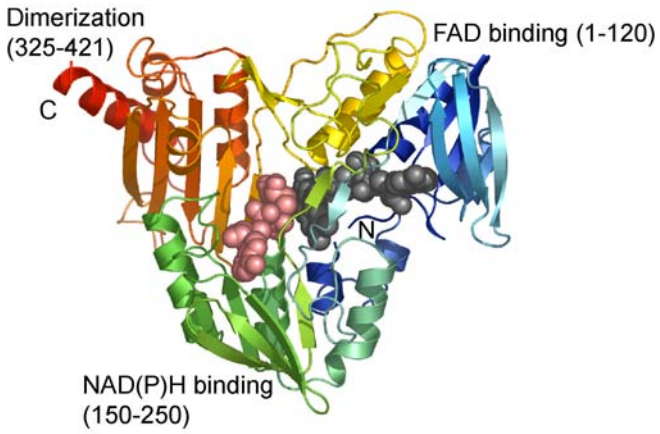

Figure 4.4: 3D structure of *L.san*-Nox2. There are two ligands shown inside the structure: ADP (red); FAD(black)

There are different *L. lactis* substrains: *Lactococcus lactis* IL1403 is the strain that is published in the NCBI database; ATCC 19435 is the *L. lactis* strain we bought from ATCC; MG1363 is the strain the Jeroen Hugenholtz group (102)used for the isolation of water-forming NADH oxidase from lysate. According to the water-forming NADH oxidase first ~25 amino acid alignment, we could see that the strains encode a different protein (Figure 4.5). In fact, it was found out that the nox2 gene between ATCC19435 and MG1363 has 93% amino acid level identity (102).

IL 1403	MKIVVIGTNHA--GIATANTL**I**D**R**YPG
ATCC19435	MKIVVIGTNHA--GIATANTL**I**D**Q**YPG
MG1363	MKIVVIGTNHAAGIATANTL**L**E**Q**YPG

Figure 4.5: Amino acid alignment among different *L. lactis* strains IL1403, ATCC19435 and MG1363. Amino acids in bold are the differences among them (1).

The nox-2 enzyme from *L. lactis* MG1363 has been obtained previously via protein purification from cell lysate (1). In this chapter, we report cloning, expression, purification, and characterization of the water-forming NADH oxidase from *L. lactis* ATCC 19435. We will focus on the comparison between nox-2 and the combined nox-1/peroxidase system with respect to their kinetic behaviors and stabilities against overoxidation.

4.2 Material and Methods

4.2.1 Cloning

The noxE genes from *L. lactis* ATCC19435 were isolated from the genomic DNA using the following gene-specific primers derived from the coding sequence: 5'ATGAAAATCGTAGTTATCGGTACG3' (noxE) and 5'TTATTTTGCATTTAAAGCTGCAAC3' (noxE).

NoxE was successfully amplified by the polymerase chain reaction (PCR) using *Taq* polymerase (Fermentas, Hanover, MD). The PCR products were then purified through gel electrophoresis and subsequent elution (Gel Extraction Kit, Qiagen, Valencia, CA). NoxE were then cloned into pDrive vector that encoded blue/white screening feature (Qiagen PCR Cloning kit, Qiagen, Valencia, CA), and transformed into XL10-Gold competent cells. Positive clones were identified as white colonies. The recombinant and pDnoxE were obtained through miniprep (Qiagen Spin Miniprep kit, Qiagen, Valencia, CA), analyzed by PCR and sequenced.

pDnoxE constructs were used as templates for the PCR of the desired genes and the PCR product were subcloned into the expression vector pET30 (EK/LIC cloning kit, Novagen, Madison, WI). The pET30 vector has a 6xHistidine tag and an S tag on its N-terminus. Plasmid pET27noxE was constructed by subcloning a *NdeI-HindIII* fragment engineered by PCR from the original pDnoxE into pET-27b(+)(Novagen, Madison, WI) that encodes a C-terminal His tag. All of the clones were successful and the recombinants were first transformed into XL10-Gold cells for positive/negative test and then recombinants pET30noxE and pET27noxE were transformed to the expression strain BL21(DE3)-RIL (Stratagene, La Jolla, CA).

4.2.2 Induction and overexpression

The successful clones pET30noxE and pET27noxE were grown in LB broth with 30 μg/mL Kanamycin and 50 μg/mL chloramphenicol at 37^{o}C for 3~4h. Protein overexpression was induced with 200~500 μM isopropyl β-D-thiogalactopyranoside (IPTG) at an OD_{600} of 0.3~0.7, overexpression were conducted at 37^{o}C, and cells were harvested after 3~4 h. The pellet was suspended in 15 mL 50mM sodium phosphate buffer at pH 7 containing 300 mM NaCl and destroyed by sonication (8 x 30 sec, 1min pause).

4.2.3 Protein purification

By taking advantage of the N- or C-terminal 6xHis tag, all of the proteins were purified by using immobilized metal affinity chromatography as described before (IMAC; BD TALON Co2+ Metal Affinity CellTru Resin, BD Biosciences, Palo Alto, CA) (65). Nox-1 and AhpC were then dialyzed overnight against pH 7.0 50mM HEPES, 1mM EDTA buffer, using a UF membrane with 12~14 kDa MWCO (Spectrum Laboratories, Rancho Dominguez, CA) and Slide-A-Lyzer MWCO 3,500 Dialysis Cassette (Pierce, Rockford, IL), respectively; buffer was changed twice. *L.lac*-Nox2 was dialyzed in the same manner as nox-1 except using pH 7, 50mM HEPES, 1mM EDTA, 5mM dithiothreitol (DTT) buffer instead. Protein concentration was measured by the Bradford assay using a Biophotometer (Eppendorf, Westbury, NY).

4.2.4 NADH-oxidase activity assay

L.lac-Nox2 activity was measured by the decrease in absorbance at 340nm, corresponding to the decrease in concentration of the substrate NADH at 30°C in a DU-800 spectrophotometer. *L.lac*-Nox2 was reconstructed with FAD and scanned over the

spectra of 250nm-750nm. Its kinetic parameters were determined with 53 μM externally added FAD.

Nox-2 activity was assayed with a DU-800 spectrophotometer (Beckman Coulter) at 30°C in a total volume of 1.5 mL air-saturated 50mM HEPES buffer at pH 7.0 and 0.24mM NADH. The reaction was initiated by the addition of a suitable amount of enzyme and the rate of NADH oxidase was monitored by the decrease in absorbance at 340nm (ε = 6220 $(M \cdot cm)^{-1}$). The measurement of kinetic parameters with substrate NADH and cofactor FAD was performed in a similar manner. Nox-2 was first incubated with 53 μM FAD at 30 °C for 10min before adding NADH. 53 μM FAD was chosen for the comparison with nox-1.

4.2.5 Absorption Spectrum

Nox-2 was scanned in the air-saturated pH 7, 50mM HEPES at 30°C in a 1.5ml quartz cuvette. The absorption spectrum (250nm-750nm) was recorded in the DU-800 spectrophotometer.

4.2.6 Activity-pH profile of nox-2

The following buffer systems were used to investigate the pH dependence of nox-2 at 30°C with 0.24mM NADH: Sodium acetate from pH 4.0 to pH 5.0; MES from pH 5.0 to pH 6.5; HEPES from pH 6.5 to 9.5. At pH 5.0 and 6.5, activity was measured in both sodium acetate and MES buffer at pH 5 and in MES and HEPES buffer at pH 6.5.

4.2.7 Effect of temperature on *L.lac*-Nox2

The temperature range of 15 °C to 60°C was chosen to measure the activity of nox-2 in pH 7, 50mM HEPES buffer with 0.24mM NADH. Both the buffer and the

substrate NADH were incubated at a chosen temperature for 10 to 20min before adding nox-2 to the reaction solution.

4.2.8 Total Turnover Number (TTN)

A specific amount of nox-2 was added to the 1.5 mL air-saturated 50mM HEPES buffer +/- 5mM DTT at pH 7.0, 30°C. NADH was added until the enzymes could no longer react.

4.2.9 Amplex Red assay for H_2O_2 on nox-2

We employed the horseradish peroxidase (HRP)-catalyzed oxidation of 9-acetylresorufin ("Amplex Red", Molecular Probes, Eugene, OR) to fluorescent resorufin as our H_2O_2 assay (65). The sample from the reactions of nox-2 with 0.26mM NADH was also tested for the hydrogen peroxide formation.

4.2.10 *L.lac*-Nox2 purification and denaturation

By taking advantage of the C-terminal His tag of *L.lac*-Nox-2, the protein was purified by using immobilized metal affinity chromatography as described before (IMAC; BD Talon Co^{2+} Metal Affinity CellThru Resin, BD Biosciences, Palo Alto, CA). *L.lac*-Nox2 was then dialyzed overnight against pH 7.0 50 mM HEPES buffer, using a UF membrane with 12-14 kDa MWCO (Spectrum Laboratories, Rancho Dominguez, CA). The protein was denatured at 100 °C for 8 min and centrifuged at 14,000rpm.

4.2.11 HPLC analysis of endogenous ligand

The collected supernatant was analyzed by a Beckman Coulter System Gold 126 solvent Module HPLC using a C_{18}-reversed phase column (Beckman Coulter, 4.6 x 250 mm). A 5 minute isocratic elution was run with 0.1M ammonium acetate, pH 5.3 followed by a 25 minute linear gradient to 50% methanol using a 1 mL/min flow rate.

The eluted peaks were monitored by absorbance at 260 and 450 nm with a Beckman Coulter System Gold 168 detector. Authentic standards of 10 μM ADP (Sigma-Aldrich, St. Louis, MO) and 10 μM FAD (Sigma-Aldrich, St. Louis, MO) were also analyzed by these conditions. To one sample of the denatured protein supernatant, 10 μM ADP was added and analyzed as above.

4.3 Results

4.3.1 DNA sequencing of *L.lac*-Nox2

The sequencing results of pET30noxE and pET27noxE show five silent mutations and four amino acid discrepancies (R22Q, L212S, S278Y, N385S) when compared to the annotated noxE gene sequence from *L. lactis* IL1403 in the NCBI database (Figure 4.6).

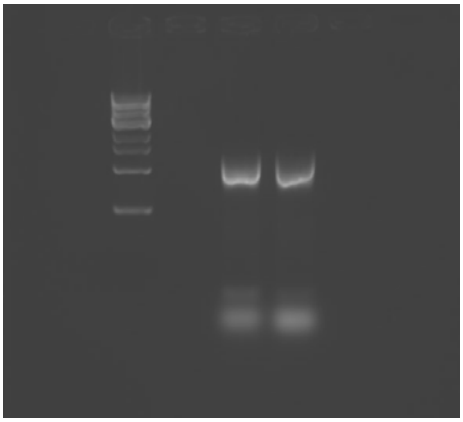

Figure 4.6: *L.lac*-Nox2 PCR products.

If the N-terminal amino acid sequences of *L. lactis* IL1403 from the NCBI database, of the strain *L. lactis* MG1363 (1), and of the ATCC19435 strain in this work are compared one finds four differences among the first 25 or 26 N-terminal amino acids (Figure 4.5). Thus, we expect that there are more differences in the overall sequence and possibly also the properties between the *L. lactis* noxes-2 from the MG1363 and ATCC19435 strains.

4.3.2 Protein expression and purity

The open reading frame for nox-2 is capable of encoding a protein with a molecular mass of 49kDa, which is in good agreement with those values previously

published on similar water-forming NADH oxidases. SDS-PAGE of the proteins derived from the expressed genes exhibited prominent bands at the expected size (Figures 4.7).

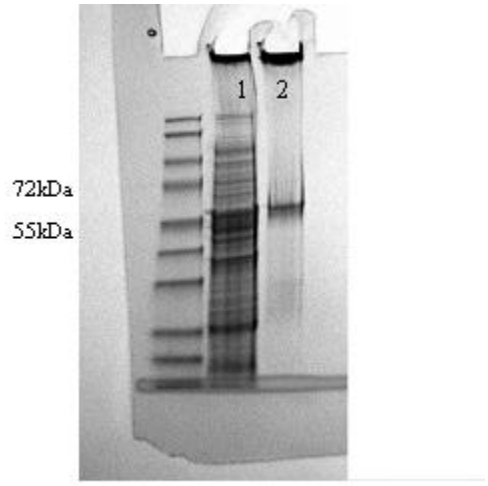

Figure 4.7: Purification of C-nox2. Lane 1: Lysate; Lane 2: protein purified

All of the protein samples collected after IMAC showed no other bands other than the protein of interest on the SDS-PAGE gels (N-terminally His-tagged nox-2 is not shown).

4.3.3 FAD/subunit

The native nox-2 in air-saturated buffer reveals a typical spectrum of a flavoprotein with absorption peaks at 380nm and 441nm. From the scan of the nox-2 (Figure 4.8), we found an absorbance ratio A_{450}/A_{280} of 0.126. The ratio of FAD associated per subunit of enzyme was calculated from the result of the Bradford test for amount of enzyme, the assumption of dimeric association of *L. lactis* nox-2 (1), and the molar absorption coefficient ε for FAD of 11,300 $(M \cdot cm)^{-1}$ (103). The calculated value of

1.86 mole of subunit per mole of FAD indicates the presence of one FAD molecule per subunit. As we reported before, nox-1 from *L. lactis* needs to be reconstituted with FAD to obtain the holo-enzyme after purification because it loses its FAD during the purification step. While nox-2 from *L. lactis* appears yellow after applying the same purification method, we still proceeded to add exogenous FAD to our nox-2 preparation (results see below).

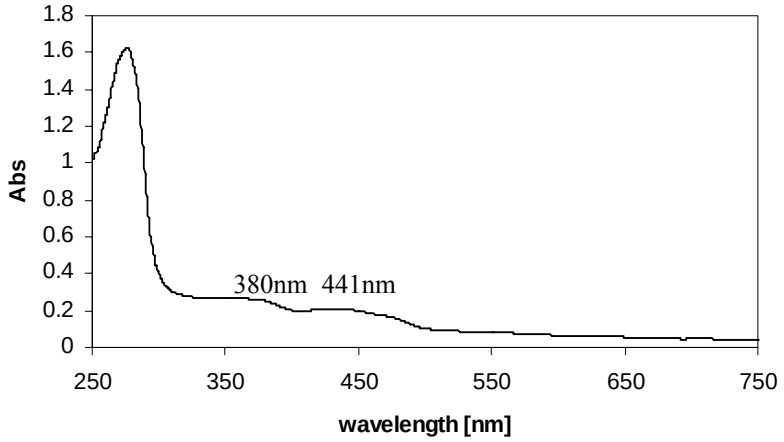

Figure 4.8: UV-vis absorbance spectrum of nox-2 from *L. lactis.* 50mM HEPES, 1mM EDTA, pH 7, 30°C. Absorbance peaks: 380 and 441nm.

4.3.4 N-*L.lac*-Nox2 Kinetics

The following figure showed the NADH saturation curve of N-terminally His-tagged *L.lac*-Nox2 (N-*L.lac*-Nox2). From Figure 4.9, we can see that N-*L.lac*-Nox2 is almost saturated at a concentration of 0.3 mM NADH. The K_M value of NADH was found to be 53 μM, the maximum velocity was 0.095 μmol/(L x s), resulting in a maximum specific activity of 23.75U/mg as evidenced by the Hanes Plot (Figure 4.10).

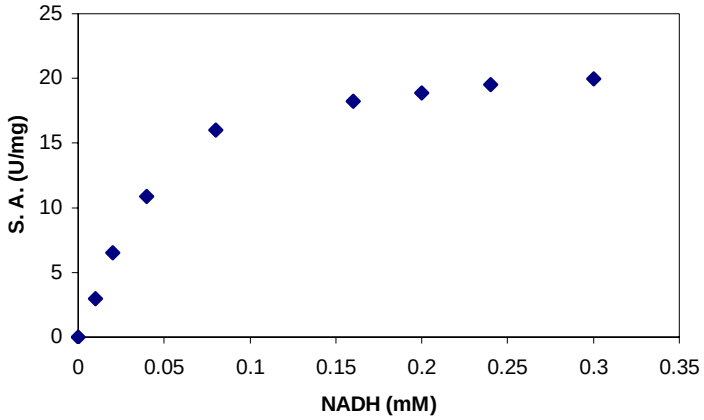

Figure 4.9: Saturation curve of N-*L.lac*-Nox2. Air saturated pH7, 50mM HEPES, 5mM DTT, 30 °C

4.3.5 N-*L.lac*-Nox2 Product inhibition from NAD^+

It was found that NAD^+ would inhibit the N-*L.lac*-Nox2. When NAD^+ concentration is below 10.67mM, NAD^+ shows non-competitive inhibition. However, when the NAD^+ concentration is above 10.67mM, NAD^+ shows a different inhibition on enzyme N-*L.lac*-Nox2. When NAD^+ concentration exceeds 22mM, it totally inhibits enzyme activity.

4.3.6 Kinetic parameters of nox-1 and nox-2

The K_M and v_{max} values as well as the maximum specific activity of C-*L.lac*-Nox2 and N-*L.lac*-Nox2 were calculated from the Hanes plot (Figure 4.10). FAD stimulates the activity of both nox-1 and nox-2. In the case of nox-1, the activity of holo nox-1 is 2.04 U/mg (0.24mM NADH), but with 53µM externally added FAD, the activity becomes seven times higher (see Chapter 3.3.6). In the case of nox-2, the externally added 53µM

FAD doubled the activity of nox-2. The comparison of kinetic parameters between nox-1 and nox-2 is shown in Table 4.1.

Table 4.1: Comparison of kinetic data of nox-1 and tagged *L.lac*-Nox-2

Enzyme	K_M (μM), NADH	v_{max} μmol/(L·s)	v_{max}/[E] (U/mg)	K_M (μM), NADH (53μM FAD)	v_{max} μmol/(L·s)	v_{max}/[E] (U/mg) (53μM FAD)
Nox-1	n.d.	n.d.	2.04	76	0.98	14.7
C-nox2	73	1.88	45.1	90	3.92	94.1
N-nox2	53	0.12	23.9	n.d.	n.d.	n.d.

n.d. = not determined; conditions: air-saturated solution, 0.24 mM NADH, pH 7.0, 50mM HEPES, 30°C, with or without 53μM of FAD.

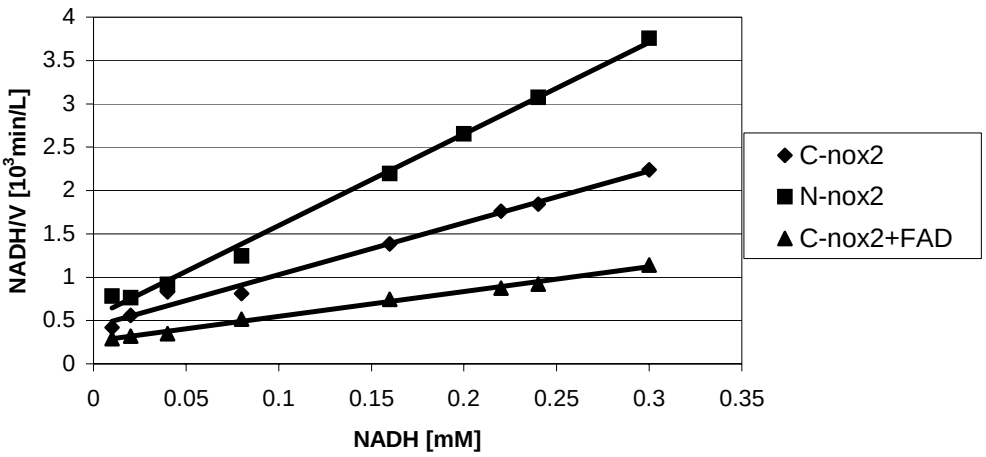

Figure 4.10: Hanes plot of kinetics of N- and C- His-tagged *L.lac*-Nox2. Air-saturated substrate NADH (0.24 mM), pH 7.0, 50 mM HEPES, 30°C, with or without 53μM of FAD.

4.3.7 pH effect on *L.lac*-Nox2

The optimum pH for nox-2 was observed to lie between pH 6.5 and pH 7.5. Rates at low pH (pH 4 to 5) are reported as net rates, with the chemical decomposition rate at low pH subtracted. Below pH 5.0, the activity of nox-2 is very low compared to its

optimum value. The sample instantly loses its activity in both acetate and MES buffer at pH 5.0. At pH values above 5.0, the activity of nox-2 increases with an optimum at pH 7.0 and followed by a gradual decrease in activity at high pH values.

Both nox-2 from *L. lactis* and nox-2 from *L. sanfranciscensis* (Figure 4.11) feature gaps in the activity-pH-profile at pH 5.0 and pH 5.5, respectively. The calculated pI values for nox-2 from *L. lactis* and *L. sanfranciscensis* are 5.66 and 5.4, respectively, and the pI value for nox-2 from *L.lactis* MG1363 was shown to be 4.8 on isoelectric focusing gels (1). Whether or not the gap is related to the proximity of the pH to the pI is under further investigation.

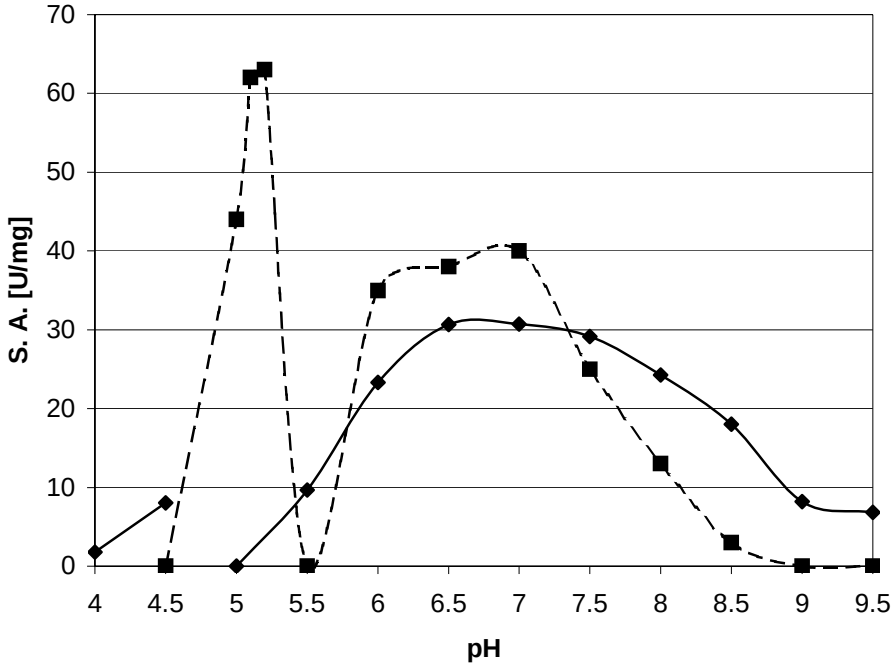

Figure 4.11: Activity-pH-profile of *L.lac*-Nox2, comparison with profile of *L. san*-Nox2 (dashed line) (66)

4.3.8 Activity profile with respect to temperature

The temperature profile shows that nox-2 reaches its optimum at 40°C in 50mM HEPES buffer at pH 7.0. Above 15°C, the activity of nox-2 gradually increases until it hits the optimum plateau between 40°C to 50°C, and decreases to zero when at 60°C. At 60°C, the enzyme was completely inactive after the first 10~20 sec reaction with substrate NADH (Figure 4.12). The activation energy E_a was calculated to be 24.8 kJ/mol from the Arrhenius plot between 15 and 40°C (picture not shown).

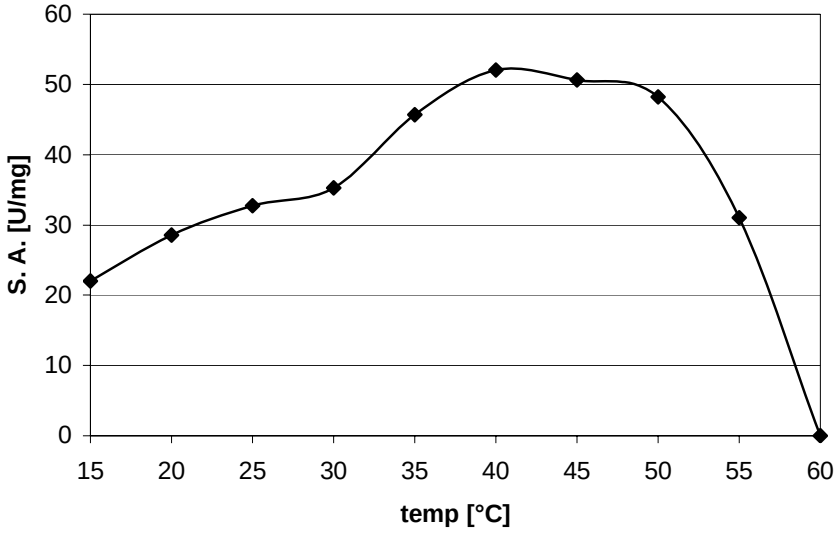

Figure 4.12: Activity-temperature-profile of *L. lac-N*ox2. Optimum temperature: 40°C.

4.3.9 Hydrogen peroxide generation

When analyzing nox-2, although nox-2 is a water-forming NADH oxidase, we found 0.4 ~ 0.7% H_2O_2 generated after its reaction with NADH. *L.san*-Nox2 was also found out to generate 0.5% hydrogen peroxide during catalysis by my colleagues. Because *L. lac*-nox2 has similar 3D structure as *L. san*-nox2, we suppose the reason of the similar percentage of H_2O_2 release is the same (Figure 4.13): Oxygen attacks the flavin C4α and forms peroxy, then FAD-C4α-peroxy is formed after interacting with the

reduced flavin (101). The nicotinamide ring prevents H_2O_2 from releasing from the *re*-face, so H_2O_2 reacts with C42 of the *si*-face and forms sulfenic acid.

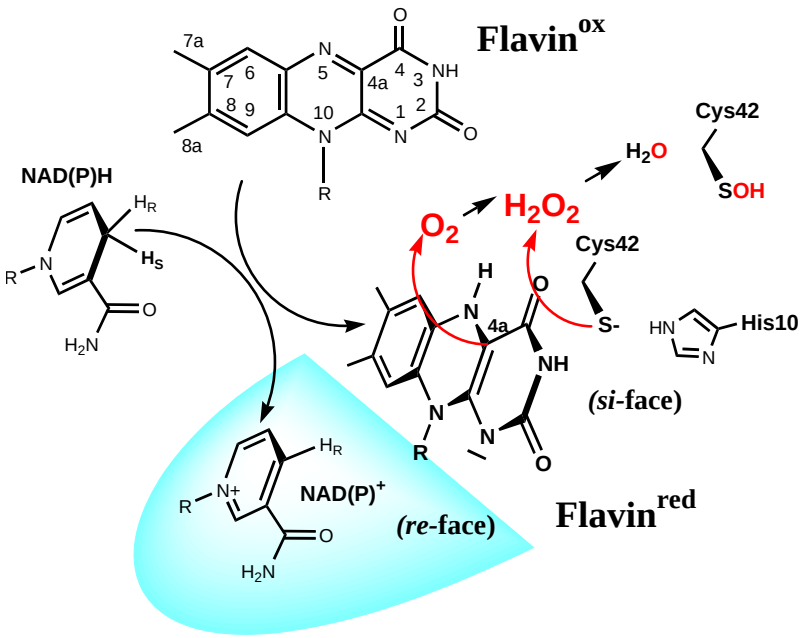

Figure 4.13: Proposed mechanism of how intermediate hydrogen peroxide reacts

4.3.10 Total Turnover Number (TTN)

The operational stability of alkyl hydroperoxide reductase and NADH oxidase is not limited by temperature but by catalytic turnover. When testing the degree of conversion, as calculated from the decrease of absorption of NADH at 340nm, at low enzyme concentration (<500pM), we observed that the reaction came to a standstill with incomplete conversion of NADH. We verified inactivation of the enzyme by spiking again with NADH, but no further conversion of NADH occurred. For the C-terminally his tagged nox-2, the TTN almost doubled upon addition of 5mM DTT to the buffer (Table 4.2).

Table 4.2 : TTNs for nox-1 and nox-2 enzymes from *L. lactis*

	TTN	AhpF/AhpC (1000:1)	AhpF/AhpC (1:1)	AhpF/AhpC (1:20)	AhpF	N-nox2	C-nox2
HEPES	82,000	82,000	82,000	82,000	n.d.	38,740
HEPES, 5mM DTT	82,000	82,000	82,000	82,000	52,000	78,480

Conditions: [AhpF] = 22nM; [C-nox-2]=30nM; [N-nox2]=51nM; n.d. : not determined

4.3.11 HPLC analysis results of the endogenous ligand

HPLC analysis of the endogenous ligand(s) released from heat-denatured *L.lac*-Nox2 indicates that only FAD binds to the enzyme as isolated (Figure 4.14), which is different from *L.san*-Nox2. The *L.lac*-Nox2 protein sample yields a single peak ADP with a retention time of 24.9 minutes at 260 nm, which was identical to the 450 nm trace (Figure B). The sample from "A" was then augmented with 10 μM ADP to yield two peaks with retention times of 13.7 and 24.8 minutes at 260 nm and one peak at 450 nm (Figure D). Authentic standards of 4 μM ADP and 10 μM FAD yield retention times of 13.4 and 24.8 minutes (Figure E), respectively.

The structures show that the NAD(P)H binding pockets in *L.san*-Nox2 are each occupied by an ADP molecule. Consequently, the A_{260}/A_{450}-ratio of 9.27 and 6.3 (from protein spectrum) for *L.san*-Nox2 and *L.lac*-Nox2, respectively, is consistent with the presence of ADP in the former, but not in latter . Therefore, substrate preference in *L.lac*-Nox2 is likely dictated by the residues lining the putative NADH-binding domain. In

contrast, the presence of the ADP ligand in *L.san*-Nox2 appears to be responsible, at least in part, for the lack of substrate preference between NADH and NADPH.

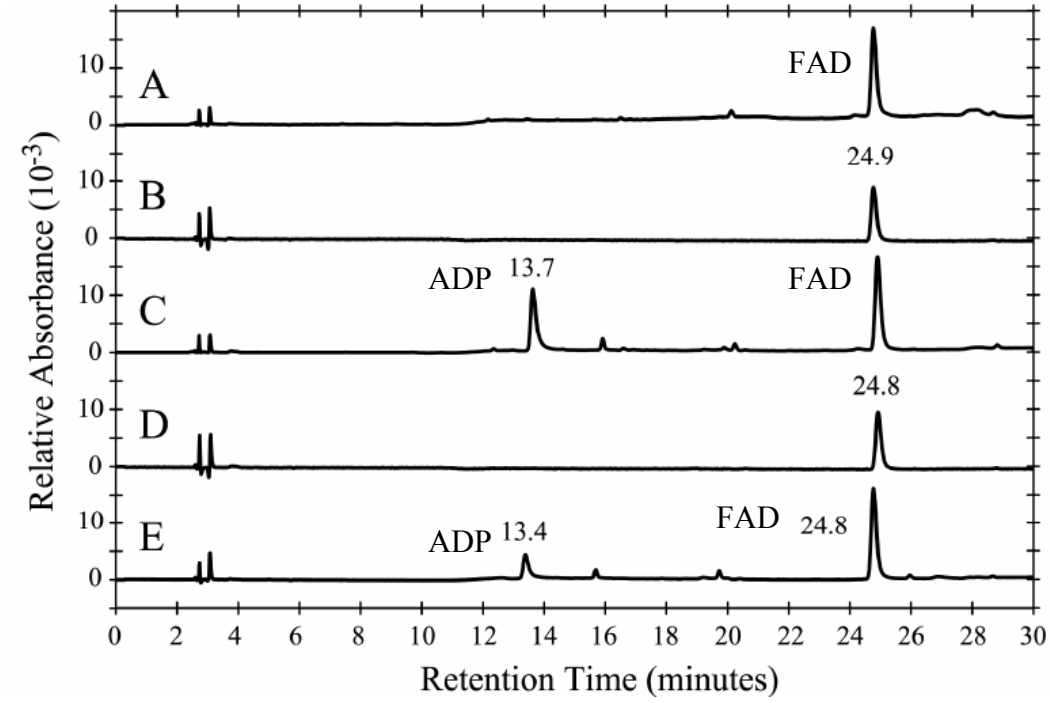

Figure 4.14: Separation of FAD from denatured *L.lac*-Nox2 by HPLC (260nm and 450nm) A,B) the supernatant from heat denatured enzyme C,D) sample from A was augmented with ADP E) authentic standards of ADP and FAD

4.4 Discussion

We have successfully applied the sequence comparison-based approach to find water-forming NADH oxidase (nox-2) genes in *L. lactis*. Upon sequencing both enzymes, we found just one silent mutation at Ser63 in the AhpC (188 amino acids) but five silent mutations and four amino acid changes in our nox-2 protein from ATCC19435 (448 amino acids) in comparison with the enzyme from the IL 1403 strain in the NCBI database (86). Moreover, the nox-2 protein purified before from the lysate of the MG1363 strain differed from ours in four amino acid positions of the 26 positions sequenced N-terminally in the former (the complete nox-2 sequence from MG1363 still does not exist). [(1)] However, none of those discrepancies is in a conserved region and the differences do not seem to impair enzyme activity significantly.

We found that externally added FAD enhances the activity in both nox-1 and nox-2 *L. lactis* enzymes to apparent maximal specific activities of 15 and 94 U/mg, respectively. In *S. mutans*, which also features both AhpF/AhpC and nox-2 (73,81), the oxidase activity of nox-1 from *S. mutans* was found to be stimulated on addition of FAD, while that of nox-2 was not. Furthermore, the activities of nox-1 from *Bacilllus megaterium* and *Thermus thermophilus* (104,105), and nox-2 from *Streptococcus faecalis* 10C1 are enhanced by FAD as well. On the other hand, work on nox-2 from *L. sanfranciscensis* and *Leuconostoc mesenteroides* found that free FAD has no effect on activity of those enzymes (87) (54,66) (106). Our calculated occupancy of nearly 1.0 upon the addition of exogeneous FAD, in comparison with about 0.5 without added FAD, points to the possibility of free FAD diffusing to an apo-flavin site of *L. lactis* nox-1 and nox-2 variants and consequently enhancing specific activity of the fully occupied holo-

enzyme. In several other nox-2 variants, FAD seems to be neither lost nor taken up, thus is probably tightly (though often non-covalently) bound; in those cases, addition of exogenous FAD predictably has no effect.

Although alkyl hydroperoxide reductase is active as a 1:1 protein complex between one molecule each of AhpF and AhpC, we found that only a vast excess of AhpC over AhpF leads to complete reduction of intermediately generated hydrogen peroxide to water. This finding points to mostly unproductive collisions between these two enzymes in solution resulting in incomplete turnover of hydrogen peroxide, although the N-terminal his tag, in contrast to a C-terminal tag, should not interfere with interactions with AhpC.

N-terminally his-tagged nox-2 has a considerably lower specific activity than its C-terminally his-tagged counterpart. The possible reason is that the N-terminal domain is the NADH binding domain, so that an N-terminal his-tag obstructs binding of NADH to the enzyme. Our C-terminally his-tagged nox-2 shows similar maximum specific activity as the untagged *L. lactis* nox-2 from MG1363 reported before (1), 94 compared to 83 U/mg, but with a much higher K_M value of 90 μM compared to 4.1 μM on the latter.

It is remarkable that we found around the same percentage of released hydrogen peroxide generated by nox-2 from *L. lactis* and *L. sanfranciscensis*, 0.4 to 0.7% of the stoichiometrically expected value, as measured by generation of resorufin from Amplex Red. This finding might point to a possible common mechanism of nox-2 enzymes to not release intermittently formed hydrogen peroxide but rather convert it into water with electrons from a second molecule of NADH. The intermittently formed hydrogen peroxide is thought to be captured by the active-site cysteine42 as a sulfenic acid (cys42-

SOH) intermediate, only a negligible amount (0.4-0.7%) is released. Electrons from a second molecule of NADH reduce the sulfenic acid to water and thiolate (cys42-S^-). We currently investigate the feasibility of such a mechanism.

While alkyl hydroperoxide reductase from *L. lactis* has lower maximum specific activity than nox-2 under same reaction conditions, its total turnover number was higher than that for the *L. lactis* nox-2. However, total turnover of *L. lac*-Nox2 is doubled in the presence of DTT, which is in agreement with results on *L.san*-Nox2 (for nox2 from *L. sanfranciscensis*, TTN is increased dramatically from 3500 to above 112,000 upon the addition of 5 mM DTT in the reaction buffer) (64).

ADP ligand was found in *L.san*-Nox2 but not *L.lac*-Nox2. *L.san*-Nox2 can take both NADH and NADPH as its substrate, while *L.lac*-Nox2 can only take NADH. Dual substrate specificity observed in *L.san*-Nox2 can be rationalized in at least two ways. One hypothesis assumes that the ADP ligand remains bound to the enzyme during turnover. Consequently, the NAD(P)H substrates may access the FAD via the large *re*-face channel observed in the structure. The nicotinamide ring from either NADH or NADPH can be appropriately positioned adjacent to the isoalloxazine ring, provided that Tyr159 is rotated out of the way. In contrast, NADH specificity in the other homologs is due, in part, to the amino acid residue located 19-21 residues downstream of the last glycine in the signature motif. In general, NADP+ specificity derives from an arginine at this position, which provides ionic and hydrogen bonding interactions with the 2'-phosphate of NADP+. In contrast, NAD^+ specificity derives from an acidic amino acid at this position, which hydrogen bonds with the 2' hydroxyl group and provides for electrostatic selection against NADPH ligands. In *L.san*-Nox2, Asp179 occupies this important

position and hydrogen bonds with the 2' hydroxyl group of the ADP molecule. In *L.lac*-Nox2, the residue is Asp177. However, the HPLC analysis of denatured *L.lac*-Nox2 indicates that it does not contain a high affinity ADP ligand. Consequently, it can be rationalized that specificity towards NADH and exclusion of NADPH in the *L.lac*-Nox2 as dictated by residues lining the putative NADH binding site. In contrast, the occupancy of ADP in *L.san*-Nox2 typical NADH-domain requires that NAD(P)H substrates must access the FAD via the larger channel, which lacks the typical interactions in the to dictate strict substrate preference.

The second hypothesis for dual substrate-specificity in *L.san*-Nox2 assumes that the ADP ligand departs during turnover, and that NAD(P)H subsequently binds in an analogous position as the observed ADP ligand. The residues lining the *L.san*-Nox2 this putative NADH binding site suggest that the enzyme may accommodate either NADH or NADPH. For example, NADH or NADPH binding could be essentially analogous to the ADP ligand observed in the current structure. This does not forecast any significant alterations to protein side chains to accommodate NADH binding, with the exception of Tyr159, which is also applicable to the NADPH binding modes as well. However, a slight conformational change of Asp179, which is possible based upon examination of alternative rotomers, would be required to move the negative charge of the side chain away from the region nearest the 2' phosphate group of a bound NADPH substrate. In further support of this binding mode, it is noted that Lys213, His181 and Lys187 are all positioned to either hydrogen bond and/or stabilize the charge of such a bound NADPH molecule. Indeed, these interactions are analogous to those in NADPH complex of glutathione reductase. In contrast and as noted above, there are no positively charged

residues within the vicinity of the 2' phosphate group of the docked NADPH in either the model for *L.lac*-Nox2 or the NADH peroxidase structure. Consequently, the structures predict that these latter enzymes should not oxidize NADPH.

4.5 Conclusions

In conclusion, we found that nox-1 (AhpF) from *L. lactis* is considerably slower than its nox-2 counterpart. Both nox-1 and nox-2 are both turnover-limited, as expected for enzymes with labile, redox-active thiols in the active site. However, as evidence by the higher total turnover numbers, nox-1 is considerably more stable against overoxidation (TTN of 82,000) than nox-2 in the absence of exogenously added thiols, such as DTT (TTN of 39,000).

Addition of exogenous thiols, such as DTT, increases nox-2 stability by a factor of two, up to the level of nox-1. In comparison, nox-2 from *L. sanfranciscensis* is much less stable than its *L. lactis* homolog without exogenous thiols but is much more stabilized in their presence. As sequence identity between nox-2 of *L. lactis* and *L. sanfranciscensis* is only 33%, amino acid composition seems to influence stability behavior. The ADP ligand was found tightly bound in the 3D structure of *L.san*-Nox2, but was not found in *L.lac*-Nox2.

Kinetic and stability analysis does not reveal any clear advantage for oxygen scavenging via the nox-1 or the nox-2 routes in lactic acid bacteria. Differences in effectiveness therefore are likely to be caused by different expression levels rather than performance per protein molecule. However, when both enzymes take oxygen as its substrate, alkyl hydroperoxide reductase system needs two enzymes (nox-1 and AhpC) to generate water as its final product, while nox-2 could be the single enzyme to accomplish this, i.e., the nox-2 is comparatively simple if used in the cofactor regeneration system. Specific activity wise, both *L.san*-Nox2 and *L.lac*-Nox2 showed higher activity than nox-1 from *L. lactis*.

CHAPTER 5

WHOLE-CELL CATALYST WITH CARBONYL REDUCTASE AND WATER-FORMING NADH OXIDASE

5.1 Introduction

Enzymes are being used increasingly widely in industrial synthetic chemistry as excellent catalysts. They are capable of catalyzing reactions exhibiting strict enantioselectivity, regioselectivity, or both under benign conditions. Both isolated enzymes and whole cells have been used industrially as catalysts. Compared with isolated enzymes, whole cell catalysts can be much more readily and inexpensively prepared. Because enzymes in cells are protected from the external environment, they are generally more stable in the long-term than free enzymes. In particular, microbial cells have been most commonly used for industrial purpose thanks to their diversity and ease of handling. For example, Mercian used the recombinant *E. coli* cell with Lysine aminotransferase (*Flavobacterium lutescenns*) for the production of L-pipecolic acid from L-Lysine (107); Company Kyowa Hakko employed Proline hydroxylase from *Streptomyces sp.* in *E.coli* for the production of hydroxyproline from proline (108).

The recombinant DNA technique has greatly increased the availability of whole-cell catalyst. It has enabled the overproduction of a desired enzyme in various heterologous hosts, and allows the use of cells containing multiple catalysts. This technique has even made it possible to modify metabolic pathways in the host cells, such as cofactor regeneration system, biosynthesis of complex metabolites, etc.

Using whole-cell system for the NAD(P)H cofactor regeneration have been well studied. There are numerous examples of cofactor regenerations in whole cell processes. These ranges from the use of baker's yeast to genetically engineered microorganisms, for example, for the oxidation of octane using monoxygenases (109). Application ranges from lab to industrial scale. Kroutil and Faber recently reported the synthesis of a variety of chiral (S)-alcohols using whole cells of *Rhodococcus ruber*. 2-propanol was used for cofactor regeneration. Muller reported the enzymatic reduction of ketoesters to yield the corresponding hydroxy esters. In this case a crude cell extract of the alcohol dehydrogenase from *Lactobacillus brevis* was used (110). Cofactor regeneration was achieved by using 2-propanol as well. In a similar way keto esters were reduced by the co-expression of an ADH and GDH in *E. coli* by Shimizu and coworkers (111). The two step enantio- and diastereoselective reduction of diketones by whole cells of *Lactobacillus kefir* has been reported by Liese and co-workers (112,113). Selectivity and yield could be controlled in a continuously operated process using a special feeding strategy. A space-time yield of 64 g/ (L x d) was achieved for (2R, 5R)-hexanediol leading to a production in kg-scale. Where poorly water-soluble substrates and products are involved, the use of XAD-resins for *in situ* substrate delivery and product extraction have been reported (114). Also the ionic liquid [BMIM][PF6] that is water-immiscible has been introduced for this purpose (115-117). Resting cells of *Geotrichum candidum* have been used for the enantioselective reduction of ketones in supercritical carbon dioxide (118).

Whereas the NAD(P)H cofactor regeneration in the whole-cell catalyst has been well investigated, the $NAD(P)^+$ regeneration in the whole-cell catalyst is less well

studied. This chapter is about the investigation of the possibility of using the E. coli whole-cell catalyst containing both L.san-Nox2 gene and carbonyl reductase from L. lactis (LL-CR) for the oxidative reactions of alcohols such as 2-hexanol (Figure 5.1). L.san-Nox2 here is for the regeneration of $NAD(P)^+$ cofactor. It was chosen because carbonyl reductase can only take $NADP^+$ and L.san-Nox2 is the only enzyme we have that can take NADPH as its cofactor--L.lac-Nox2 is NADH-specific.

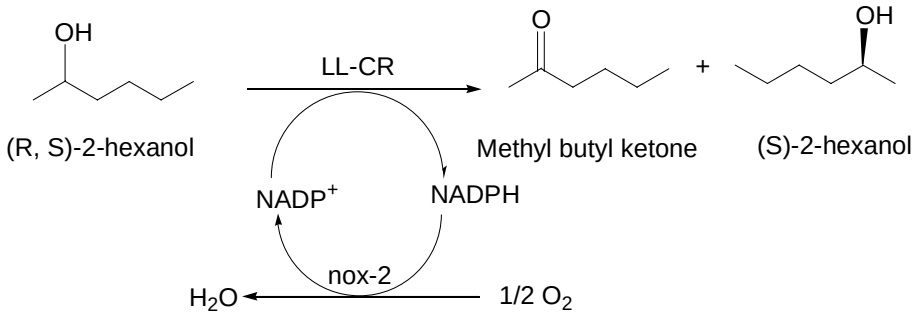

Figure 5.1: *In situ* cofactor regeneration with (R)-LL-CR and nox-2: (R)-LL-CR catalyzes the oxidation of (R,S)-2-hexanol to methyl butyl ketone and (S)-2-hexanol.

Carbonyl Reductase (secondary-alcohol: $NADP^+$ oxidoreductase, EC 1.1.1.184) belongs to the family of short chain dehydrogenase/reductases (SDR) (119,120). They are ubiquitous in nature and catalyze the NADPH reduction of a large number of biologically and pharmacologically active substrates, including a variety of endogenous and xenobiotic carbonyl compounds (121). Carbonyl reductases are mostly monomeric, cytosolic enzymes that reduce aldehyde and keto groups of prostaglandins, steroids, pterins, biogenic amines, and quinines derived from polycyclic aromatic hydrocarbons (122). It could be found in non-mammalian tissue of plants (123), bacteria (124), yeast (125), fish and insects (126,127).

Carbonyl reductase was found to contain a Rossmann fold with the conserved GlyXXXGlyXGly sequence in the amino terminal part of the enzyme that is involved in

cofactor binding. Another conserved sequence is Tyr at position 194 that is part of a common TyrXXXLys sequence found in SDR active sites (128).

Carbonyl reductase from *Candida magnoliae* and *Candida macedoniensis* can be coupled with NADPH-regenerating glucose dehydrogenase in *E. coli* to catalyze the reduction reaction of ethyl 4-chloro-3-oxobutanoate (COBE) to ethyl-4-chloro-3-hydroxybutanoate (CHBE) (Figure 5.2) (129,130). Carbonyl reductase from *Kluyveromyces aestuarii* was also found to produce (S)-4-chloro-3-hydroxybutanoate (ECHB) with formate dehydrogenase, which is to regenerate NADPH cofactor (131). We are going to use the coupled enzymes—LL-CR and *L.san*-Nox2—for the oxidation of alcohols such as 2-hexanol. This is the opposite reaction of what the other research groups have done, i.e. we are going to prepare an *in situ* cofactor regeneration system in *E. coli* for oxidative reaction, not reductive reaction.

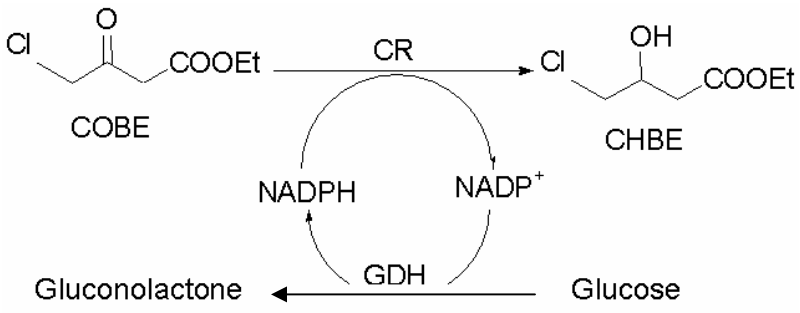

Figure 5.2: *In situ* cofactor regeneration with CR and GDH

Carbonyl reductase from *L. lactis* (LL-CR) is also a member of the short-chain dehydrogenase family. Some research work has been done on LL-CR in our lab but not published yet. The pure LL-CR is an annotated identical tetramer with 30kDa per subunit. The enzyme acts on (R)- but not on (S)-secondary alcohols, thus is (R)-specific. The optimum pH is around 6.5. Just like other carbonyl reductases, it is also a

NADP(H) dependent enzyme, which can take a wide range of alcohols or ketones as its substrate, such as 1,2-propanediol, diethylene glycol, isopropanol, 1-butanol and acetophenone. It has higher activity towards the production of alcohols than the formation of ketones. The specific activities of LL-CR towards alcohols are less than 1U/mg and its activity towards ketones varies from 0.4 U/mg to 8 U/mg. Nox-2 catalyzes an irreversible reaction of oxygen to water, so the carbonyl reductase reaction towards ketone can be increased when coupling with nox-2.

Two ways of coexpressing two heterogeneous genes in *E. coli* cells were found in literature: two-plasmid-two-gene system and one-plasmid-two-gene system

i) The two-plasmid-two-gene system was found to be successful in the asymmetric reduction of COBE to CHBE by cloning aldehyde reductase gene (AR) from *Sporobolomyces salmonicolor* to pKK223-3 vector and glucose dehydrogenase (GDH) gene from *Bacillus megaterium* to pACYC vector (132). Carbonyl reductase gene from *Candida macedoniensis* was cloned into pET21a and GDH gene was cloned into pACYC in *E. coli* BL21 (DE3) for the CHBE production (133). When transforming two plasmids to E. coli cells, these two plasmids must have different but compatible replicons. Otherwise, one of the plasmids will be "kicked out" of the cell.

ii) one-plasmid-two-gene system is used in the production of L-amino acids, such as L-Leucine, L-valine and L-tyrosine with *E. coli* TG1 cells, containing both L-amino acid dehydrogenase and formate dehydrogenase genes (134). One-plasmid-two-gene system can also be used for the reduction

of COBE to CHBE, using pKK223-3 coexpressing the AR gene (*Sporobolomyces salmonicolor*) and GDH gene (*Bacillus megaterium*) in *E. coli* JM 109 (132). Here, the expression vector must have two multiple cloning sites for the cloning of two genes.

There is no conclusion about which system is better overall, i.e., showing higher enzyme activity and higher expression level. Both of these two systems will be constructed and investigated in my work. The vectors chosen for the expression of LL-CR and *L.san*-Nox2 are pETDuet-1 and pACYCDuet-1. The copy number of pETDuet-1 is about 40 and that of pACYCDuet-1 is around 12, so pETDuet-1 will be used to express LL-CR and pACYCDuet-1 will be chosen to express *L.san*-Nox2 in the two-plasmid-two-gene system in BL21(DE3). Thus, the activity level between these two enzymes could be balanced inside the cell. For the one-plasmid-two-gene system, pETDuet-1 is chosen to express both LL-CR and *L.san*-Nox2 with different expressing sequence.

5.2 Materials and Methods

5.2.1 Materials

Diethyl ether and acetone are purchased from EMD Chemicals (Gibbstown, NJ). 2-Hexanone and dihydro-4,4-dimethyl-2,3-furandione are purchased from Sigma Aldrich (Milwaukee, WI). 2-Hexanol is from Acros Organics (NJ, USA). Potassium phosphate monobasic is from Fisher (Rockwood, TN, USA) and cyclohexanone is from Mallinckrodt (Hazelwood, MO). The enzymes, vectors, marker DNA, marker proteins, oligonucleotides and other reagents used for cloning experiments were purchased from Qiagen (Germany), New England Biolabs (USA), Invitrogen (Netherlands), Novagen (Madison, USA) and MWG (Highpoint, USA).

5.2.2 Cloning and transformation

E. coli strain BL21 (DE3) (Novagen) was used as host organism. pKK-nox2 was kindly donated by Bettina R. Riebel from Emory University. Plasmid pNC containing both nox-2 and LL-CR in the expression vector pETDuet-1 (Novagen) were constructed as follows and their structures are given in Figure 5.3. For construction of pNC-1, primer P1 5' GCATATCCATGGGTAAAGTTATTGTAGTAGGTTGTACT3' (restriction sites are underlined) and primer P2 5'GCATATAAGCTTTTATTTATGTGCTTTGTCAGCTTGT3' were used to subclone the nox-2 gene to the *Nco I-Hind III* site. pKK-nox2 was used as a template for the PCR. The other two primers P3 (5'-GCATATAGATCTCATGAAAACACTTATCACTGGCGA-3') and P4 C5'-GCATATCTCGAGTTATTTTTTAAATTTACGCTTTAAACCATTTTTAGC-3' were used to subclone the LL-CR gene to the *Bgl II-XhoI* site. The gene was obtained from

genomic DNA of *L lactis*. The construction of pCN was carried out in a similar way with pETDuet-1 using different primers. Nox-2 was cloned to the *Bgl II-XhoI* site using primer P5 (N5'-GCATATAGATCTCATGAAAGTTATTGTAGTAGGTTGTACT-3') and primer P6 (C5'-GCATATCTCGAGTTATTTATGTGCTTTGTCAGCTTGT-3') primers and LL-CR was cloned to *Nco I-Hind III* site using primer P7 (N5'-GCATATCCATGGGTAAAACACTTATCACTGGCGA-3') and primer P8 (C5'-GCATATAAGCTTTTATTTTTTAAATTTACGCTTTAAACCATTTTTAGC-3'). The pACnox2 plasmid was constructed by cloning nox2 gene to the *Bgl II-XhoI* site of pACYCDuet with primers P5 and P6 and LL-CR was cloned to the *Nco I-Hind III* site to make pET-LL-CR, using primers P7 and P8.

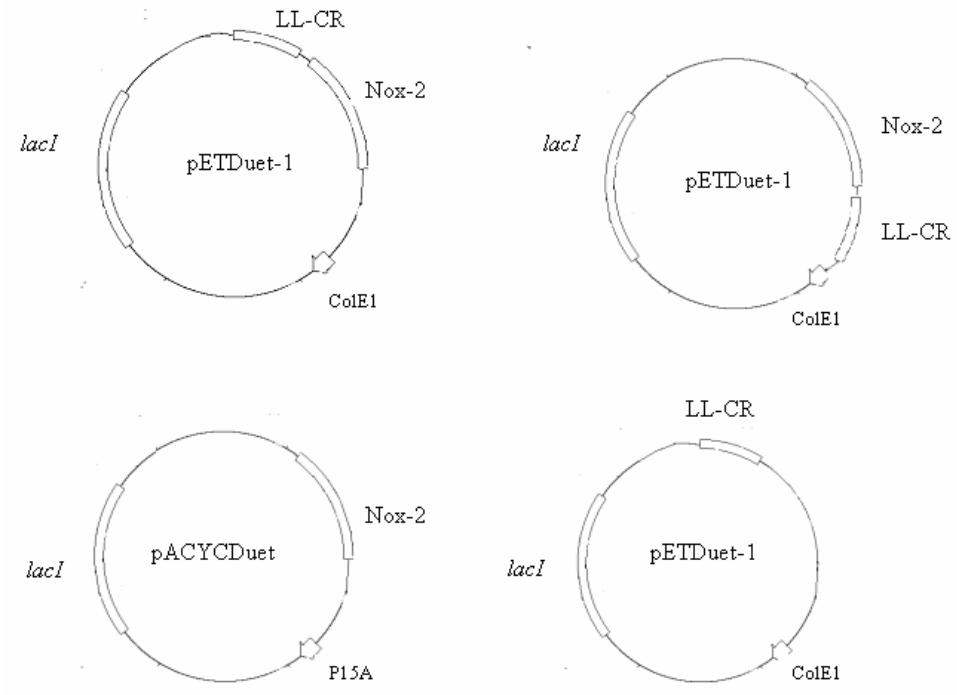

Figure 5.3: One-plasmid-two gene system and two-plasmid-two-gene system. One-plasmid system using pETDuet-1: pNC and pCN. Two-plasmid system using pACYCDuet-1 (P15A) and pETDuet-1 (ColE I): pNox and pCR

5.2.3 Coexpression of carbonyl reductase and NADH oxidase

For co-expression of both CR-LL and NADH oxidase in *E. coli* cells, two compatible recombinant plasmids pACnox2 and pET-LL-CR, were simultaneously introduced into *E. coli* BL21(DE3) cells. pNC and pCN were introduced into BL21(DE3) cells, respectively.

5.2.4 IPTG Induction

Cells were inoculated with overnight culture and were collected after growing in 500 mL LB broth with 50 μg/mL ampicillin and 30 μg/mL chloramphenicol at 37^{o}C, 180 rpm for 3~4h. Protein overexpression was induced with 200~500 μM isopropyl β-D-thiogalactopyranoside (IPTG) at OD_{600} around 0.5. Protein overexpression were conducted at 37 ^{o}C, and cells were harvested after 4~6 h.

5.2.5 Preparation of cell-free extracts

The cells were suspended in 10 mL 50 mM potassium phosphate buffer (pH 7.0) buffer and then disrupted with an ultrasonicator (Fisher Scientific). After centrifugation at 5,000 rpm for 20 min, the resulting supernatant was used for the enzyme assay and some biotransformations.

5.2.6 Bioconversion with recombinant *E. coli*

The reaction mixture comprising, in 100 mL, 100 mM pH 7.0 potassium phosphate buffer, 0.12 mM $NADP^{+}$ and 30 mM dextrose and cells of the transformant (obtained from 500 mL culture) was incubated with 20 mM 2-hexanol at 37 ^{o}C 180 rpm in the orbital shaker. Samples were talem at different time points during the process and extracted with 3x20 mL diethyl ether before analysis by GC.

5.2.7 Bioconversion with lysate

The reaction mixture comprising, in 100 mL 100 mM pH7 potassium phosphate buffer, 0.12 mM $NADP^+$ and 1 mM DTT and pCN cell lysate (obtained from 500 mL culture) was incubated with 20 mM 2-hexanol/2-hexanone/ 20 mM cyclohexanone at 37 C 180 rpm in the orbital shaker. Samples were taken at different time points during the process and extracted with 3x20 mL diethyl ether before analysis by GC.

5.2.8 GC method

The concentration of the substrate/product in the reaction mixture was measured by the GC-flame ionization detector (GC-FID, HP6890 Series). The following GC method was applied: Isothermal at 70 ^oC for 15 min followed by a temperature increase of 40 ^oC /min to a final temperature of 220 ^oC, which was maintained for 5 min. Acetone was used as the solvent for dissolving 2-hexanol/2-hexanone/cylcohexaone standards.

5.2.9 NADH oxidase activity assay

Nox-2 activity in the lysate was measured by the decrease in absorbance at 340nm, corresponding to the decrease in concentration of the substrate NAD(P)H (ε = 6220 $(M \cdot cm)^{-1}$) at 30 °C in a DU-800 spectrophotometer (Beckman Coulter). The reaction solution contains 50 mM HEPES (pH 7.0), 1 mM DTT, 0.24 mM NAD(P)H.

5.2.10 Carbonyl reductase activity assay

LL-CR activity in the lysate was measured by the tracking of absorbance at 340nm with a DU-800 spectrophotometer in a total volume of 1.5 mL air-saturated 50mM HEPES buffer (pH 7.0) at 30°C. The reaction solution contains either 1 mM DTT, 0.24 mM NAD(P)H and 20 mM 2-hexanol or 1 mM $NADP^+$ and 20 mM Acetophenone.

5.3 Results

5.3.1 Sequencing results

Mutations were found in LL-CR in the expression vectors: E8A, V29I, K52E and 9 silent mutations. None of the mutations were highly conserved comparing to other short-chain dehydrogenase. *L.san*-Nox2 was found to have the following mutations in the expression vectors: A30V and one silent mutation G116 (GGT to GGC). However, V30 is also found in *Streptococcus mutans* nox-2 and *S. pyogenes* nox-2 enzymes, so it is possible that the reason for the A30V mutant is the difference of our *L. lactis* strain with the *L. lactis* strain in the NCBI database.

5.3.2 Overexpression of carbonyl reductase and NADH oxidase

Both *L.san*-Nox2 and LL-CR are overexpressed with pETDuet-1 and pACYCDuet-1 vectors (Figure 5.4). In the one-plasmid-two-gene system, when using pETDuet-1 to coexpress two enzymes together, it was found the gene in MCS I was expressed much better than the one in MCS II. In the two-plasmid-two-gene system, both *L.san*-Nox2 and LL-CR are overexpressed.

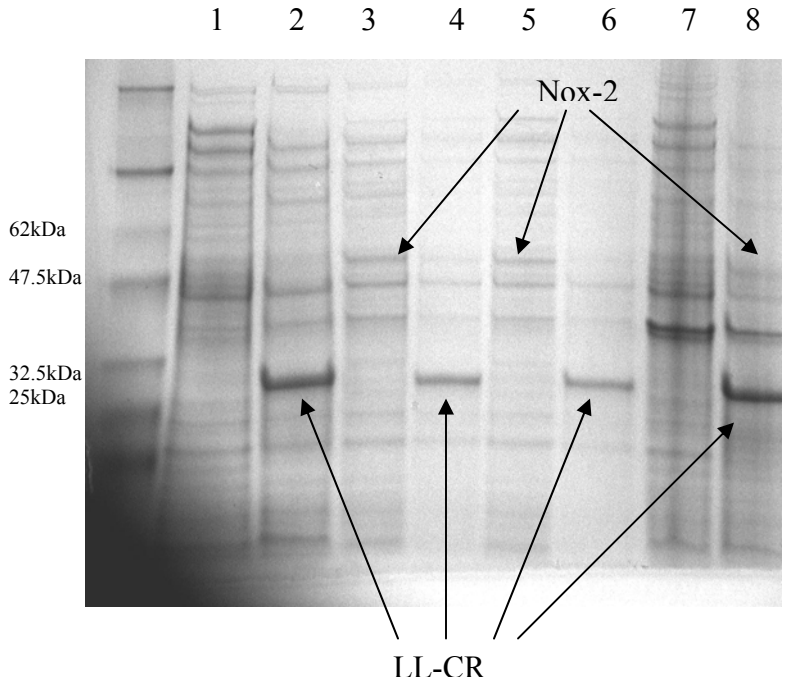

Figure 5.4 : SDS-PAGE of *L.san*-Nox2 and LL-CR.
Lane 1: BL21(DE3) Lysate
Lane 2: pACYC-nox2 + pETDuet-LL-CR (soluble)
Lane 3: pETDuet-nox2(soluble)
Lane 4: pETDuet-LL-CR(soluble)
Lane 5: pETDuet-nox2-LL-CR(soluble)
Lane 6: pETDuet-LL-CR-nox2(soluble)
Lane 7: BL21 (DE3) (insoluble)
Lane 8: pACYC-nox2 + pETDuet-LL-CR (insoluble)

5.3.3 NADH oxidase activity in lysate

In terms of *L.san*-Nox2 activity in different recombinant *E. coli* lysate, the order is as following: pETDuet-nox2 > pETDuet-LL-CR-nox2 > pETDuet-nox2-LL-CR> pACYC-nox2 + pETDuet-LL-CR> pETDuet-LL-CR ~BL21 (DE3) (Table 5.1). This order shows the level of *L.san*-Nox2 expression under different conditions. With pETDuet-nox2 expresses the largest amount of *L.san*-Nox2 among all of the recombinant *E. coli* cells, it shows the highest activity. Because pETDuet-LL-CR does not have the

L.san-Nox2 gene, the lysate showed the L.san-Nox2 activity close the control BL21(DE3) cells.

Table 5.1: *L.san*-Nox2 activity with NADPH/NADH in lysate

Lysate	S. A. (U/mg) NADH	S. A. (U/mg) NADPH
BL21 (DE3)	0.082	0.02
pETDuet-nox2	0.83	0.41
pETDuet-LL-CR	0.10	0.02
pETDuet-nox2-LL-CR	0.23	0.05
pETDuet-LL-CR-nox2	0.27	0.08
pACYC-nox2 + pETDuet-LL-CR	0.14	0.033

5.3.4 Carbonyl reductase activity towards alcohols in lysate

LL-CR showed extremely low activity when it catalyzed the alcohol oxidation to ketone. Table 5.2 showed its activity towards 1,2-propanediol, diethylene glycol, 1-butanol and 2-hexanol. Control BL21 (DE3) showed high activity in all of the reactions of alcohol to ketone except the 2-hexanol case. This could be caused by other unknown enzymes in *E. coli* cells, such as alcohol dehydrogenase, that catalyzed the oxidative reaction of alcohols. With all of the alcohol substrates, when LL-CR and L.san-Nox2 are both in present, after the reaction reaches steady state, the absorbance at 340 nm was constant. This means that both LL-CR and *L.san*-Nox2 are active in the lysate.

Table 5.2: Carbonyl reductase activity in lysate

S. A. (U/mg)	1, 2-propanediol	Diethylene Glycol	1-Butanol	2-hexanol
LL-CR only	5×10^{-4}	5×10^{-5}	2×10^{-6}	4.8×10^{-5}

5.3.5 Bioconversion of 2-hexanol and 2-hexanone

Among all of the recombinant *E. coli* cells we obtained, pCN showed the highest activity of the combination of *L.san*-Nox2 and LL-CR. Thus pCN was chosen for the bioconversion of 2-hexanol. As shown in Table 5.3, BL21(DE3) cell consumes 2-hexanol by itself slowly during the bioconversion process. pCN takes 2-hexanol as its substrate but only generated very tiny amounts of 2-hexanone as its product (from GC graph, not shown). The reason is that pCN probably has some unknown enzymes that take 2-hexanone right after it is generated. Table 5.4 shows that when 2-hexanone was the substrate for bioconversion, it was totally consumed after 3 hours. BL21(DE3) cell lysate also can take 2-hexanone with some unknown enzymes in the lysate.

In conclusion, 2-hexanol is not a good substrate for the bioconversion purpose because some unknown enzymes in the pCN lysate and BL21 (DE3) lysate would consume both the substrate and its product 2-hexanone.

Table 5.3: Bioconversion of 2-hexanol with pCN and BL21(DE3) lysate

pCN		BL21(DE3) control
t	2-hexanol Left (%)	2-hexanol Left (%)
0	100	100
3	47.9	60
6	40	52
22	0	51

Table 5.4: Bioconversion of 2-hexanone with pCN and BL21(DE3) lysate

pCN		BL21(DE3) control
t	2-hexanone Left (%)	2-hexanone Left (%)
0	100	100
3	0	66
6	0	44
22	0	8.7

5.3.6 Bioconversion of cyclohexanone

After finding out 2-hexanol is not a good substrate for the whole-cell catalyst, we wanted to see if cyclohexanol would be a proper substrate for the bioconversion process. Its product cyclohexanone was tested first to see if pCN would consume cyclohexanone and take cyclohexanone as its carbon source. Table 5.5 shows that cylohexanone was not in presence after 19hr and BL21(DE3) it self will consume cyclohexanone as the carbon source as well. In conclusion, cyclohexanol is not a good substrate for the whole-cell catalyst because its product cyclohexanone would be consumed by *E. coli* cells and could not be collected after bioconversion.

Table 5.5: Bioconversion of cyclohexanone with pCN and BL21(DE3) lysate

pCN		BL21(DE3) control
t	Cylohexanone Left (%)	Cylohexanone Left (%)
0	100	100
4	63	61.3
19	0	51.2
23	0	42.5

5.4 Conclusions

Both LL-CR and *L.san*-Nox2 genes were successfully cloned to the pETDuet-1 and pACYCDuet-1 vectors in the both cases of one-plasmid-two-gene system and two-plasmid-two-gene system. The overexpression of LL-CR and *L.san*-Nox2 were visible on the SDS-PAGE gel. *L.san*-Nox2 showed the following activity order in each lysate: pETDuet-nox2 > pETDuet-LL-CR-nox2 > pETDuet-nox2-LL-CR> pACYC-nox2 + pETDuet-LL-CR> pETDuet-LL-CR ~BL21 (DE3). LL-CR lysate showed extremely low activity towards 2-hexanol.

Among all of the recombinant *E. coli* cells we obtained, pCN showed the highest activity of the combination of *L.san*-Nox2 and LL-CR. Thus pCN was chosen for the bioconversion of 2-hexanol. However, it was found out that both pCN and BL21(DE3) cells have some unknown enzymes that consumes the product 2-hexanone. The alternative substrate cyclohexanol, its product cyclohexanone was also found consumed by pCN and BL21 (DE3). The unknown enzymes and metabolic pathways are the main reasons for the unsuccessful whole-cell catalyst application. The low activity of LL-CR towards alcohol could be another problem during bio-conversion. Carbonyl reductase usually favors the reaction of ketone to alcohol, but not alcohol to ketone. All of the carbonyl reductases cloned in the whole-cell catalyst for the reductive reactions were found to have lysate activity at the level of hundred units per milligram. It's considered very important to find a highly active carbonyl reductase for the construction of a cofactor regeneration whole-cell catalyst.

CHAPTER 6

ENZYME MEMBRANE REACTOR WITH HORSE-LIVER ALCOHOL DEHYDROGENASE AND NADH OXIDASE

6.1 Introduction

A couple of membrane technology applications were applied in the chemical and pharmaceutical industry, such as reverse osmosis, a pressure-driven process for retaining low molecular weight substances. For enzyme separation from the reaction mixture, it is the state of the art to use filtration cells that are equipped with cellulose ultrafiltration membranes, to separate the biocatalyst from the crude product. The ultrafiltration membrane has a certain molecular weight cut off (10kDa here), so it will keep the enzymes in the reactor chamber while allowing small molecules like substrate and product to pass through the membrane to the upper reactor chamber. The enzyme membrane reactor (EMR) is an established mode for running continuous biocatalytic processes, ranging from laboratory units of 3 mL volume through pilot-scale units (0.5-500L) to full-scale industrial units of several cubic meters volume and production capacities of hundreds of tons per year. On the pilot and full plant scale, the reactor is usually operated properly because it has been studied and designed well in the lab (135). EMR are applied in different reactions, such as hydrogenations, ketone reductions, dihydroxylations, diethylzinc additions and Diels-Alder reactions catalyzed by chemo-or biocatalysts.

The following picture (Figure 6.1) is the EMR used for the coupled reaction of HL-ADH and NADH oxidase. The feed solution is drawn from the flask by a pump. The stream next flows into the sterile pre-filter. Here, any large particles are first removed by a coarse fiberglass filter stage, and then potential contaminants are removed by the primary filter. The pre-filter contains a ventilation port, which may be kept closed at all times since this experiment runs at relatively low pressures.

The reactor itself (Figure 6.2) is a stainless steel, jacketed vessel equipped with an internal stirring disk (coated with Teflon). The vessel is situated on a powered magnetic stirrer that drives the disk and keeps the contents of the reaction chamber well-mixed. The jacket surrounding the reaction vessel is connected to the water bath. Feed enters through the bottom of the reactor. Directly above the reaction chamber is a 47 mm diameter cellulose filter, which allows for penetration by molecules with a molecular mass of 10 kDa or lower. The samples were collected from the reactor's upper chamber.

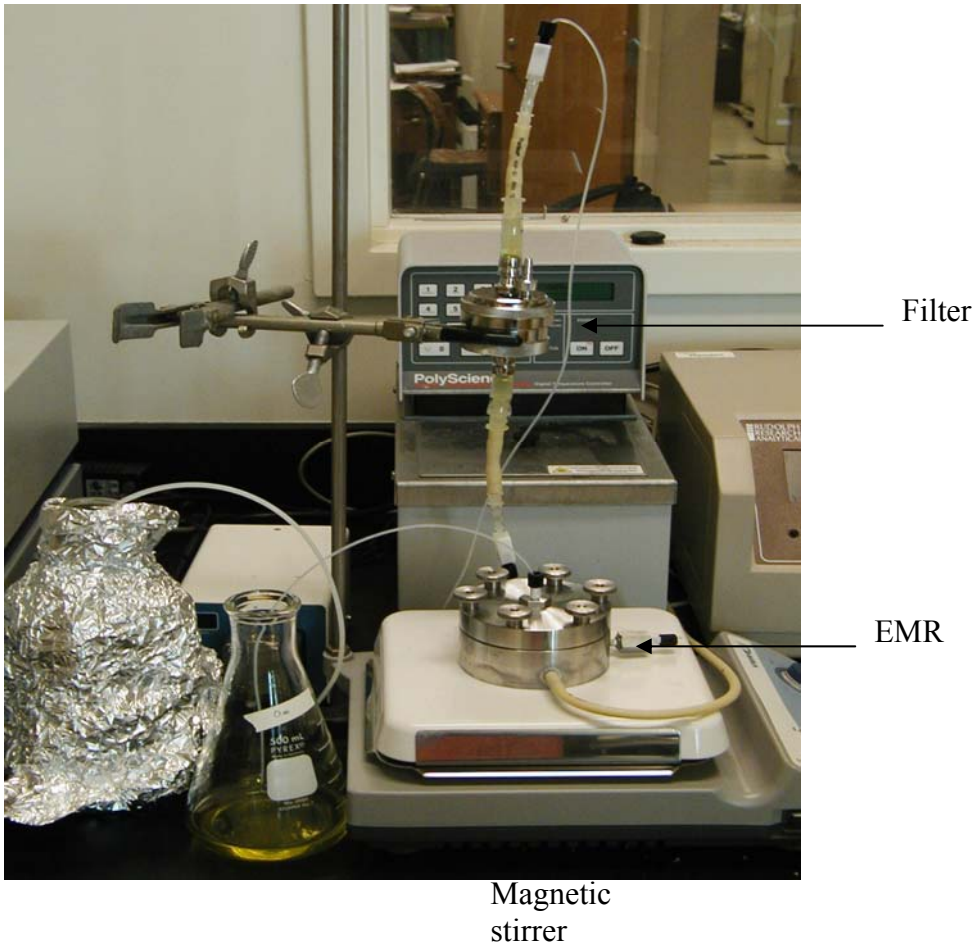

Figure 6.1: Enzyme membrane reactor for the coupled HL-ADH and water-forming NADH oxidase reactions.

Membrane reactors allow an option for the separation of biocatalysts from substrates and products. Size-specific pores of the membrane allow the relatively small substrate and product molecules to pass, but not the enzyme molecules. Membrane reactors can be operated as CSTRs (136). When it is operated as a CSTR, it will reach steady state after five times residence time.

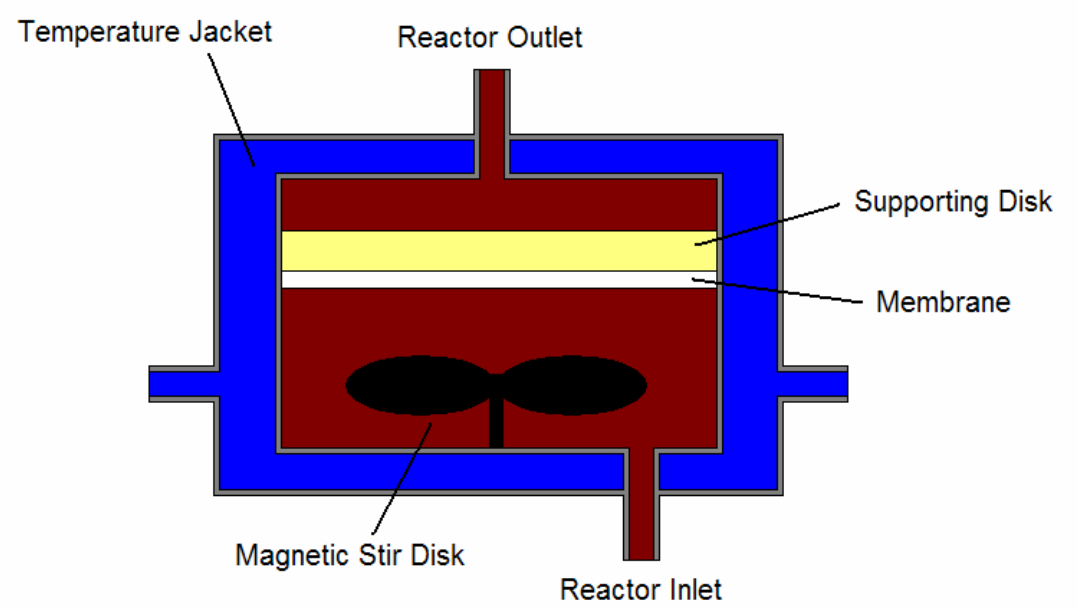

Figure 6.2: Enzyme membrane reactor vessel.

Enzyme membrane reactor was first introduced by Degussa in 1982, in which soluble enantioselective L-aminoacylase from *Aspergillus oryzae* fungus, catalyzes the N-acetyl-DL-methionine by acylase I (aminoacylase) (Figure 6.3). N-acetyl-L-methionine gets consumed and yields L-methionine whereas N-acetyl-D-methionine does not react. This process now can produce several hundred tons of L-methionine per year (137) .

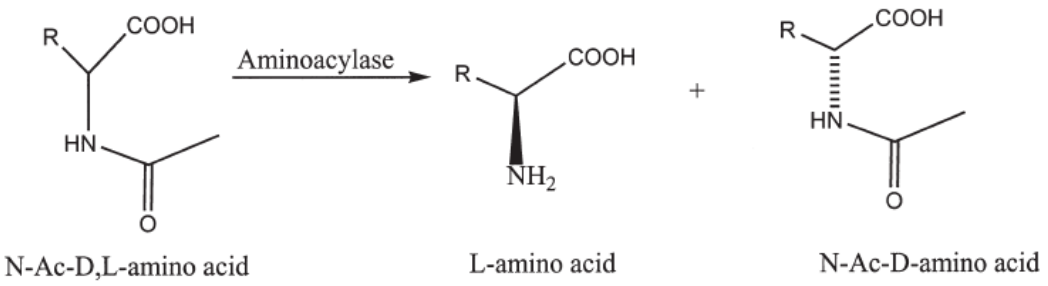

Figure 6.3: L-Aminoacylase catalytic reaction.

Enzyme membrane reactor was also applied on a large scale with the cofactor regeneration reaction (Figure 6.4). Wandrey and Kula have developed a regeneration scheme of NAD^+ to NADH using formate as reductant of NAD^+ generated upon reductive amination. The formate is oxidized irreversibly to carbon dioxide by formate dehydrogenase (138) (139). The reaction was coupled with reductive amination of alpha-keto acid substrate catalyzed by an L-amino acid dehydrogenase. With a substrate concentration of 0.5 M, L-tert-leucine was produced continuously in a membrane reactor with an average conversion of 85% and a space-time yield of 638 g/(L x day). The total turnover number over a period of two months was 125, 000 (40).

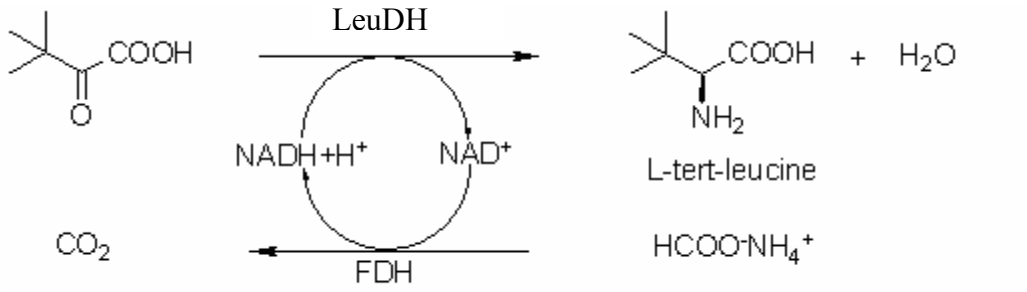

Figure 6.4: L-tert-leucine production with LeuDH and FDH.

The crucial advantages of membrane reactor are the absence of mass transfer limitations, no activity loss upon immobilization, easy addition of fresh enzyme and convenient scale-up. We are going to use ultrafiltration membranes (UF-membranes, MWCO 10kDa) that are suitable for retention of enzymes. Besides its function as a retainer, the membrane also serves other functions such as to support purification and sterilization of air and other nutrients in fermentations.

Both horse-liver alcohol dehydrogenase (HL-ADH) and *L.lac*-Nox2 are applied in EMR (Figure 6.5). HL-ADH catalyzes the oxidation of cyclohexanol to cyclohexanone while reduce NAD^+ to NADH. *L.lac*-Nox2 takes that NADH and oxygen as substrate and regenerates NAD^+ for the production reaction. The reaction catalyzes by HL-ADH was a reversible reaction. But with the coupled irreversible reaction of *L.lac*-Nox2, the equilibrium will move towards the cyclohexanone formation direction. The EMR will be operated as a continuously stirred tank reactor, i.e., the concentration, reaction rate and temperature will be the same throughout the reactor vessel. NAD^+ and cyclohexanol will be fed to the EMR continuously because the molecular weight cut of the membrane is 10 kDa.

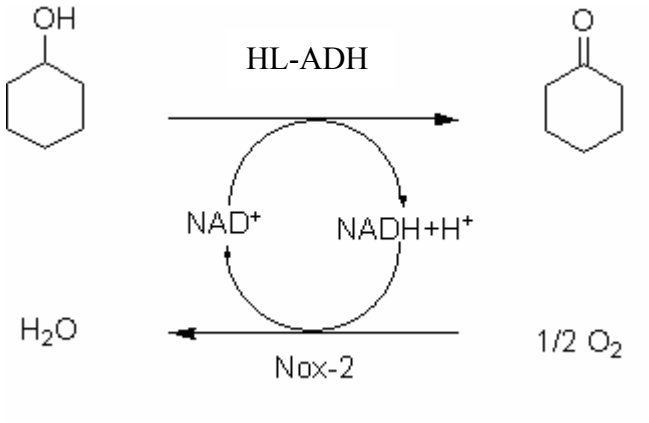

Figure 6.5: Cofactor regeneration with HL-ADH and Nox-2 enzymes

NAD^+-dependent horse-liver alcohol dehydrogenase catalyzes the oxidation of primary and secondary alcohols and the reduction of aldehydes and ketones with relatively broad specificity and is one of the most extensively studied enzymes (140). HL-ADH has a molecular weight of 40 kDa per subunit and it has metal Zn^{2+} as its cofactor. It can endure high alcohol concentration and has long life in reactions. In one study, halogenated propargylic ketones were reduced with high enantioselectivities in the

presence of HL-ADH and *Lactobacillus brevis* ADH. The enzymes were still >80% active after 15 h in ethanol and 2-propanol, respectively and TTN for the cofactor reached up to 20, 000 (38). The new technology cross-linked enzyme crystals (CLECs) helps to keep the cofactor while crystallizing. HL-ADH-NADH-CLEC preparation has maintained about 90% of the activity and can keep the activity for about three months. When using this system to reduce cinnamaldehyde, the TTN was found to be larger than 12, 000 (141). These findings are very promising for a large-scale application in the future.

Horse-liver alcohol dehydrogenase, which catalyzes the reversible oxidation of primary and secondary alcohols, exhibits very broad substrate specificity. In contrast to alcohol dehydrogenase from yeast (YADH), which exclusively accepts (S)-(+)2-butanol, (S)-(+)-2-octanol, HL-ADH also accepts the (R)-enantiomers of these alcohols and 3-pentanol which it is not a substrate for the yeast enzyme (142). HL-ADH was found to accept the following substrates: isopropanol, 3-pentanol, (S)-2-butanol, (R)-2-butanol, (S)-2-pentanol, (R)-2-penatanol (143). HL-ADH can also accept the ketone form of the following alcohols: acetone, 3-pentanone, 2-butanone, 2-pentanone. The kcat value of its activity towards different alcohols ranges from 0.6 to 2.3 s-1 while its kcat values towards ketones are usually much lower (143).

Catalyst stability is an essential feature in all processes. Thermal stability has been determined by measuring storage stability of the enzyme in conditions of temperature and pH. The choice of pH will be determined according to optimum pH ranges of both HL-ADH and *L.lac*-Nox2: HL-ADH has its optimum pH around 7.0, *L.lac*-Nox2 has its optimum at 6.5-7.0. So the pH for both of them can be chosen around

7.0. Additionally, the reaction temperature also needs to be decided by balancing enzyme activity and deactivation towards temperature. The reaction temperature should be lowered to decrease the rate of enzyme deactivation, even though enzyme catalytic activity will decrease as a consequence. The starting temperature will be 30 °C.

Operational stability is determined by parameters such as residence time. Total turnover number is also a parameter to measure the stability of the catalyst. With two enzymes in the reactor, we want to measure the TTN of *L.lac*-Nox2. Because the reactor is operated as a CSTR, the reaction rate throughout the reactor is the same, i.e., for every enzyme molecule inside the reactor, the reaction rate of each active site is the same. So we can use the integration method to get the total amount of product produced and then get the TTN of enzyme. The total activity of HL-ADH should be much larger than *L.lac*-Nox2, so that the whole system is actually dependent on *L.lac*-Nox2, i.e., the total turnover number of *L.lac*-Nox2 is the determinant factor how long the EMR could operate.

6.2 Materials and Methods

6.2.1 Materials

EMR is purchased from Juelich Fine Chemicals (Germany). NAD^+, NADH and horse-liver alcohol dehydrogenase were purchased from Sigma Aldrich. Cyclohexanol and cyclohexanone were purchased from Mallinckrodt.

6.2.2 Continuous Production of cyclohexanone

The continuous production of cyclohexanone was performed in a 10-mL stainless-steel enzyme membrane reactor (EMR) with an ultrafiltration membrane (MWCO 10kDa). The reactor was continuously mixed by a magnetic stirrer. 70% ethanol was initially pumped into the reactor to sterilize the reactor. DI water was then pumped into the reactor to remove ethanol. Enzymes were pumped into the reactor like the substrate solution. After enzymes are pumped, the substrate solution, 0.6 mM nicotinamide cofactors, with or without 53 μM FAD, 9 mM cyclohexanol in pH 7.0 100 mM PPB buffer, was continuously fed to the reactor. The reactor was continuously operated for 24~48 hours. Reactor output samples were analyzed using gas chromatography. The interval time between samples is around 1~3 hours. Every sample was checked at 340 nm.

6.2.3 GC Analysis

The concentrations of the substrate/product in the reaction mixture were measured by the GC-flame ionization detector (GC-FID, HP6890 Series). The following GC method was applied: Isothermal at 70 ^oC for 15 min followed by a temperature increase of 40 ^oC /min to a final temperature of 220 ^oC, which was maintained for 5 min. Ethyl

ether was used as the solvent for dissolving cyclohexanol/cyclohexanone standards. The standards were prepared the same way as the substrate solution.

6.2.4 HL-ADH activity

HL-ADH activity was measured by the increase of absorbance at 340nm, corresponding to the increase in concentration of the byproduct NADH (ε = 6220 $(M \cdot cm)^{-1}$) at 30 °C in a DU-800 spectrophotometer (Beckman Coulter).

6.2.5 *L.lac*-Nox2 activity

L.lac-Nox2 activity was measured by the decrease of absorbance at 340nm, corresponding to the decrease in concentration of the byproduct NADH (ε = 6220 $(M \cdot cm)^{-1}$) at 30 °C in a DU-800 spectrophotometer (Beckman Coulter).

6.3 Results and Discussion

6.3.1 Horse-liver alcohol dehydrogenase stability

Horse-liver alcohol dehydrogenase was found stable during the experiment time 48 hours. Only 0.6 mM NAD^+ was added in the feeding solution. The reason for this is that in the coupled reaction with both NADH oxidase and HL-ADH, oxygen is the limited reactant in the solution. The air-saturated reaction solution only has 0.26 mM oxygen, so it could produce 0.52 mM cyclohexanone at most, i.e. the system would take 0.52 mM nicotinamide cofactor at most. As shown in Figure 6.6, the production of cyclohexanone started at 0.08 mM and slowly decreases over time. Absorbance values (340nm) of samples taken at different time point also showed the decrease of NADH concentration overtime. The turnover number of HL-ADH during the operation time is 47. It's clear that HL-ADH could remain active for a longer time than 48 hours, but to serve as a control experiment, 48 hours is enough for our purpose.

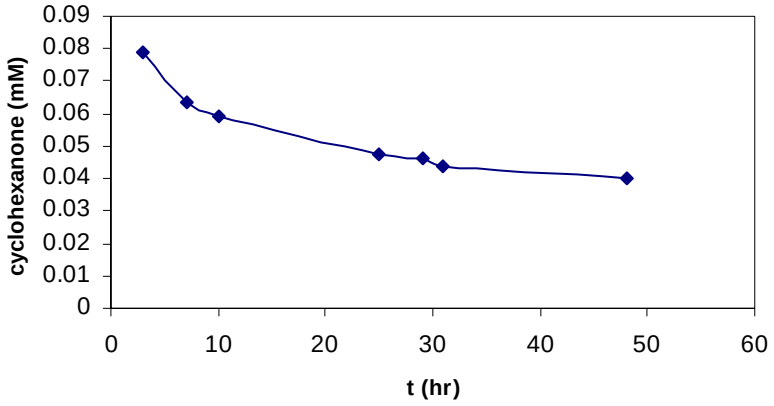

Figure 6.6: Cyclohexanone yield with HL-ADH. 0.25 μmol HL-ADH, pH 7.0 100 mM PPB, 0.6 mM NAD^+, 9 mM cyclohexanol.

6.3.2 Coupled enzyme system

To check out if addition of *L.lac*-Nox2 would increase the conversion rate, the same amount of HL-ADH (0.5 µmol, as in 6.3.1) and 5 nmol *L.lac*-Nox2 was added to the EMR for the coupled reaction, the total production of cyclohexanone in the first 20 hours was 0.04 mmol for the coupled enzyme system, comparing to 0.014 mmol of the HL-ADH only system (Figure 6.6 & 6.7). The reason for this is as following: HL-ADH catalyzes the reversible oxidative reaction of cyclohexanol; when *L.lac*-Nox2 was added, the irreversible catalysis of oxygen to water drives the equilibrium of HL-ADH towards the cyclohexanone formation direction and increases the conversion rate.

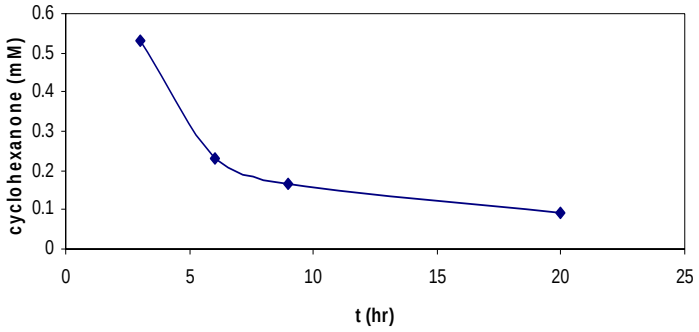

Figure 6.7: Production of cyclohexanone increased by adding *L.lac*-Nox2. 0.25 µmol HL-ADH, 5 nmol *L.lac*-Nox2, pH 7 100mM PPB, 0.6 mM NADH, 9 mM cyclohexanol, 53µM FAD, air saturated solution

6.3.3 Total turnover number of *L.lac*-Nox2

When the total HL-ADH activity is larger than that of *L.lac*-Nox2, every NAD^+ molecule converted by *L.lac*-Nox2 will be converted to cyclohexanone. NADH is in the feeding solution to the EMR. When all of the L.lac-Nox2 in the reactor stops being active, then there will be no NAD^+ available in the reactor and HL-ADH will stop

producing cyclohexanone. This also means that we can keep tracking of cyclohexanone production to know the total turnover number of *L.lac*-Nox2. As shown in figure 6.8, the production of cyclohexanone decreases very quickly in the first seven hours. This is supposed to be caused by the deactivation of *L.lac*-Nox2 because HL-ADH only deactivates slowly during the first 20 hours (see 6.3.1). The turnover number of HL-ADH is 23 in this coupled enzyme reaction, which is less than the turnover number of HL-ADH in 6.3.1. This means that the reason why the system stopped producing cyclohexanone after twenty hours is *L.lac*-Nox2 was "dead" after twenty hours, not HL-ADH. So the total turnover number of the system is NADH oxidase dependent. The total turnover number of *L.lac*-Nox2 was found to be 11,732, which is about one third that we found before (see Table 4.2). This could be caused by the mechanical force applying on enzyme at the interface caused by the stirring in the reactor. Proteins in mixed bioreactors would experience turbulent shear stress which might elicit decreased protein stability and activity. Such a situation may significantly reduce their biotechnological potential. It could be that the shear stresses injure the protein active sites and destabilize the protein. Another assumption is that the mechanical stress can provoke aggregate formation. When proteins are aggregated, the stability of the protein decreases.

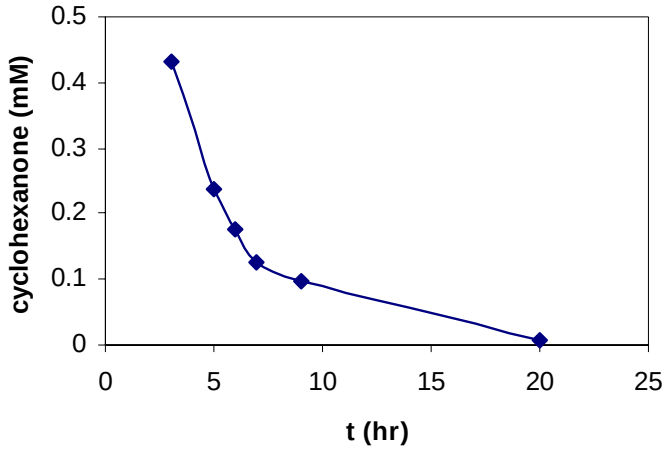

Figure 6.8: Cyclohexanone production with HL-ADH and *L.lac*-Nox2. 0.5 µmol HL-ADH, 2 nmol *L.lac*-Nox2, pH7 100mM PPB, 0.6 mM NADH, 9 mM cyclohexanol, 53µM FAD, air saturated solution

6.4 Conclusion

L.lac-Nox2 was successfully coupled with HL-ADH in the enzyme membrane reactor for the oxidation of cyclohexanone from cyclohexanol. The overall reaction rate of the coupled enzyme system was found quicker than HL-ADH alone. When 5 nmol *L.lac*-Nox2 was added to the reactor with 0.25 μmol HL-ADH, the total amount of product cyclohexanone increased from 0.014mmol to 0.04 mmol in the first 20 hours. HL-ADH was found stable in EMR. The control experiment of 0.25 μmol HL-ADH showed that it has a turnover number of 47 after 48 hours operation time. With NADH in the feeding solution, the coupled reaction of HL-ADH/*L.lac*-Nox2 would stop producing cyclohexanone if *L.lac*-Nox2 is not active anymore. It was found that the total turnover number of *L.lac*-Nox2 was 11, 732, which is less than that of *L.lac*-Nox2 in the batch reactor.

CHAPTER 7

CONCLUSION

Nicotinamide cofactors are cofactors for more than one hundred oxidoreductases. One of the obstacles of applying these oxidoreductases is the high price of these cofactors. The solution to this problem is to have in situ cofactor regeneration system. The cofactor could be regenerated biologically, chemically, phot-chemically and electrochemically. But the criterion of high reaction rate and turnover number eliminates all of the methods except the biological method. In this thesis, the focus in on novel NADH oxidase from *Lactococcus lactis*, which is a good choice for $NAD(P)^+$ regeneration. It takes oxygen as its substrate and generates water as its final product. The reaction is an irreversible one, so when it is coupled with a reversible reaction, NADH oxidase could drive the equilibrium towards the product formation direction.

There are two kinds of NADH oxidases: one is the hydrogen peroxide forming NADH oxidase, the other is the water forming NADH oxidase. Hydrogen peroxide forming NADH oxidase is part of the alkyl hydroperoxide reductase. Alkyl hydroperoxide reductase is composed of two enzymes: hydrogen peroxide forming NADH oxidase and peroxidase. Both alkyl hydroperoxide reductase and water forming NADH oxidase genes from *Lactococcus lactis* were amplified and cloned to expression vectors. All of the NADH oxidases were found to be flavoproteins. Externally added FAD can increase the activity of all of the NADH oxidases from *L. lactis*, but not the water-forming NADH oxidase from *Lactobacillus sanfranciscensis*. This also means the FAD is tightly bound to *L.san*-Nox2, but loosely bound to the Nox from *L. lactis*. Thiol

reagent DTT can increase the total turnover number of both *L.san*-Nox2 and *L.lac*-Nox2—it doubles the total turnover number of *L.lac*-Nox2 and increases the TTN of *L.san*-Nox2 by twenty folds. Both *L.san*-Nox2 and *L.lac*-Nox2 produces 0.5% hydrogen peroxide during the catalysis. When nox-1/peroxidase ratio is 1:1, the alkyl hydroperoxide reductase system produces the same amount of hydrogen peroxide as nox-1 only. Only when nox-1/peroxidase ration is 1:200, there is no hydrogen peroxide detected by the Amplex Red assay. ADP ligand was found in the 3-D structure of L.san-Nox2, but not in *L.lac*-Nox2. *L.san*-Nox2 can take both NADH and NADPH as its substrate, but *L.lac*-Nox2 can only take NADH as its substrate. It is supposed that ADP ligand could be the reason that *L.san*-Nox2 could take NADPH as its substrate while *L.lac*-Nox2 cannot.

When using the *E. coli* whole-cell catalyst containing both the carbonyl reductase gene (*L. lactis*) and *L.san*-Nox gene for the oxidation of 2-hexanol, both enzymes were found overexpressed with expression vectors pETDuet and pACYCDuet. Carbonyl reductase showed extremely low activity in the lysate towards substrate 2-hexanol. Bioconversion with the lysate solutions from BL21 (DE3) *E. coli* cells showed *E. coli* could consume that product 2-hexanone cells itself. The same result was found with another potential product cyclohexanone. So using whole-cell catalyst with both carbonyl reductase gene and *L.san*-Nox gene for the oxidation of 2-hexanol was not successful due to the unknown metabolic pathways in *E. coli* that consumes product 2-hexanone and the low activity of carbonyl reductase.

Isolated enzyme horse-liver alcohol dehydrogenase and *L.lac*-Nox2 were applied in enzyme membrane reactor. HL-ADH was found stable over an operation time of 48

hours. When HL-ADH is coupled *L.lac*-Nox2 for the oxidation of cyclohexanol to cyclohexanone, the yield was found three times higher than using HL-ADH alone, so *L.lac*-Nox2 increases the conversion rate of HL-ADH when they are coupled. The total turnover number of *L.lac*-Nox2 in EMR was found to be 11,732, which is about one third of that of *L.lac*-Nox2 in a batch reaction. The decrease in TTN could be caused by the shear stress at the interface in the well-stirred reactor.

REFERENCES

1. Felipe, F. L. d., and Hugenholtz, J. (2001) *International Dairy Journal* **11**, 37-44

2. Anderson, B., Hansen, M. M., Harkness, A. R., Henry, C. L., VInzenzi, J., and Zmijewski, M. (1995) *Journal of the American Chemical Society* **117**, 12358

3. Kragl, U., Klein, T., Vasic-Racki, D., Kittelmann, M., Ghisalba, O., and Wandrey, C. (1996) *Ann N Y Acad Sci* **799**, 577-583

4. Oppenheimer, N. J., and Kaplan, N. O. (1974) *Biochemistry* **13**, 4675-4685

5. Johnson, S. L., and Tuazon, P. T. (1977) *Biochemistry* **16**, 1175-1183

6. Kaplan, N. O., Colowick, S. P., and Barnes, C. C. (1951) *Journal of Biological Chemistry* **191**, 461-472

7. Schlenk, F., v. Euler, H., Heiwinkel, H., Gleim, W., and Nystrom, H. (1937) *Z. Physiol. Chem.* **247**

8. Guilbert, C. C., and Johnson, S. L. (1977) *Biochemistry* **15**, 335-344

9. Lowry, O. H., Passonneau, J. V., Schulz, D. W., and Rock, M. K. (1961) *J Biol Chem* **236**, 2746-2755

10. Wong, C.-H., and Whitesides, G. M. (1981) *Journal of the American Chemical Society* **103**, 4890-4899

11. Kaplan, N. O. (1960) *Pyridine Co-enzymes*

12. Adler, E., Hellstrom, H., and v. Euler, H. (1936) *Z. Physiol. Chem.* **242**, 225-249

13. Warburg, O., Christian, W., and Griese, A. (1935) *Biochemische Zeitschrift*, 157-205

14. Miwa, M., Tanaka, M., Matsushima, T., and Sugimura, T. (1974) *Journal of Biological Chemistry* **249**, 3475-3482

15. Everse, J., Anderson, B., and You, K. S. (1982) *The Pyridine Nucleotide Coenzymes*

16. Gerlach, D., Pfleiderer, G., and Holbrook, J. J. (1965) *Biochemische Zeitschrift* **343**, 354-359

17. Burgner, J. W., and Ray, W. J. (1984) *biochemistry* **23**, 3620-3626

18. Parker, D. M., Lodola, A., and Holbrook, J. J. (1978) *Biochemical Journal* **173**, 959-967

19. Kaplan, N. O., CIotti, M. M., and Stolzenbach, F. E. (1954) *Journal of Biological Chemistry* **211**, 419-429

20. Burton, K., and Wilson, T. H. (1953) *Biochemical Journal* **54**, 86-94

21. Olson, J. A., and Anfinsen, c. B. (1953) *Journal of Biological Chemistry* **202**, 841-856

22. Boyer, P. D. (1975) *The enzymes* **11**

23. Bergmeyer, H. U. (1986) *Methods of Enzymatic Analysis* **9**

24. Perry, L. J., and Wetzel, R. (1984) *Science* **226**, 555-557

25. Fersht, A. R., Shi, J. P., Wilkinson, A. J., Blow, D. M., Carter, P., Waye, M. M. Y., and Winter, G. P. (1984) *Angewandte Chemie* **96**, 455-462

26. Kaiser, E. T., and Lawrence, D. S. (1984) *Science* **226**, 505-511

27. Wilson, M. E., and Whitesides, G. M. (1978) *Journal of the American Chemical Society* **100**, 306-307

28. Ulmer, K. M. (1983) *Science* **219**, 4585

29. Lee, L. G., and Whitesides, G. M. (1985) *Journal of American Chemical Society* **107**, 6999-7008

30. Chenault, H. K., and Whitesides, G. M. (1987) *Applied Biochemistry and Biotechnology* **14**, 147-197

31. Williams-Ashman, H. G., and Banks, J. (1954) *Archives of biochemistry and biophysics* **50**, 513-515

32. Hakala, M. T., Glaid, A. J., and Schwert, G. W. (1956) *The Journal of Biological Chemistry* **221**, 191-209

33. Vrtis, J. M., White, A. K., Metcalf, W. W., and van der Donk, W. A. (2001) *J Am Chem Soc* **123**, 2672-2673

34. Devaux-Basseguy, R., Bergel, A., and Comtat, M. (1997) *Enzyme and Microbial Technology* **20**, 248-258

35. Hummel, W. (1999) *Trends in Biotechnology* **17**, 487-492

36. Donk, W. A. w. d., and Zhao, H. (2003) *Current Opinion in Biotechnology* **14**, 421-426

37. Costas, A. M., White, A. K., and Metcalf, W. W. (2001) *J Biol Chem* **276**, 17429-17436

38. Schubert, T., Hummel, W., and Muller, M. (2002) *Angewandte Chemie* **41**, 634-637

39. Bommarius, A. S., Schwarm, M., Stingl, K., Kottenhahan, M., Huthmacher, K., and Drauz, K. (1995) *Tetrahedron: Asymmetry* **6**, 2851-2888

40. Woltinger, J., Drauz, K., and Bommarius, A. S. (2001) *Applied Catalysis A: General* **221**, 171-185

41. Kelly, R. M., and Kirwan, D. J. (1977) *Biotechnology and Bioengineering* **19**, 1215-1218

42. Jaegfeldt, H., Tortensson, A., and Johansson, G. (1978) *Analytica Chimica Acta* **97**, 221-228

43. Aizawa, M., Coughlin, R., and Charles, M. (1975) *Biochimica et Biophysica Acta, General Subjects* **385**, 362-370

44. Jaegfeldt, H., Torstensson, A. B. C., Gorton, L. G. O., and Johansson, G. (1981) *Analytical Chemistry* **53**, 1979-1982

45. Laval, J. M., Bourdillon, C., and Moiroux, J. (1984) *Journal of the American Chemical Society* **106**, 4701-4706

46. Jaegfeldt, H. (1980) *Journal of Electroanalytical Chemistry and Interfacial Electrochemistry* **110**, 295-302

47. Moiroux, J., and Elving, P. J. (1978) *Analytical Chemistry* **50**, 1056-1062

48. Watanabe, H., and Hastings, J. W. (1982) *Molecular and Cellular Biochemistry* **44**, 181-187

49. Drueckhammer, D. G., and Wong, C. H. (1985) *Journal of Organic Chemistry* **50**, 5387-5389

50. Bernofsky, C., and Swan, M. (1973) *Analytical Biochemistry* **53**, 452-458

51. Schulman, M. P., Gupta, N. K., Omachi, A., Hoffman, G., and Marshall, W. E. (1974) *Analytical Biochemistry* **60**, 302-311

52. Chambers, R. P., Ford, J. R., Allender, J. H., Baricos, W. H., and Cohen, W. (1974) *Enzyme Engineering*, 195-202

53. Julliard, M., and Le Petit, J. (1982) *Photochemistry and Photobiology* **36**, 283-290

54. Riebel, B. R., Gibbs, P. R., Wellborn, W. B., and Bommarius, A. S. (2003) *Adv. Synth. Catal.* **345**, 707-712

55. Odman, P., Wellborn, W. B., and Bommarius, A. S. (2004) *Tetrahedron: Asymmetry* **15**, 2933-2937

56. Ozols, R. F., and Marinetti, G. V. (1969) *Biochemical and Biophysical Research Communications* **34**, 712-719-718

57. Everse, J., Barnett, R. E., Thorne, C. J., and Kaplan, N. O. (1971) *Archives of biochemistry and biophysics* **143**, 444-460

58. Romano, M., and Cerra, M. (1969) *Biochimica et Biophysica Acta* **177**, 421-426

59. Chambers, R. P., Walle, E. M., Baricos, W. H., and Cohen, W. (1978) *Enzyme Engineering* **3**, 363-369

60. Lemiere, G. L., Lepoivre, J. A., and Alderweireldt, F. C. (1985) *Tetrahedron Letters* **26**, 4527-4528

61. Hatanaka, A., Kajiwara, T., and Tomohiro, S. (1974) *Agricutural and Biological Chemistry* **38**, 1819-1833

62. Lamed, R. J., and Zeikus, J. G. (1981) *Biochemical Journal* **195**, 183-190

63. Hummel, W., and Riebel, B. (1996) *Annals of the New York Academy of Sciences* **799**, 713-716

64. Jiang, R., Riebel, B. R., and Bommarius, A. S. (2005) *Adv. Synth. Catal.* **347**, 1139-1146

65. Jiang, R., and Bommarius, A. S. (2004) *Tetrahedron: Asymmetry* **15**, 2939-2944

66. Riebel, B. R., Gibbs, P. R., Wellborn, W. B., and Bommarius, A. S. (2002) *Adv. Synth. Catal.* **344**, 1156-1168

67. Geueke, B., Riebel, B., and Hummel, W. (2003) *Enzyme and Microbial Technology* **32**, 205-211

68. Poole, L. B. (2005) *Arch Biochem Biophys* **433**, 240-254

69. Tartaglia, L. A., Storz, G., and Ames, B. N. (1989) *J Mol Biol* **210**, 709-719

70. Poole, L. B., Reynolds, C. M., Wood, Z. A., Karplus, P. A., Ellis, H. R., and Calzi, M. L. (2000) *European Journal of Biochemistry* **267**, 6126-6133

71. Chae, H. Z., Robison, K., Poole, L. B., Church, G., Storz, G., and Rhee, S. G. (1994) *Proc Natl Acad Sci U S A* **91**, 7017-7021

72. Poole, L. B., Higuchi, M., Shimada, M., Calzi, M. L., and Kamio, Y. (2000) *Free Radical Biology & Medicine* **28**, 108-120

73. Niimura, Y., and Massey, V. (1996) *The Journal of Biological Chemistry* **271**, 30459-30464

74. Poole, L. B. (1996) *Biochemisty* **35**, 65-75

75. Poole, L. B., and Ellis, H. R. (1996) *Biochemisty* **35**, 56-64

76. Niimura, Y., Nishiyama, Y., Saito, D., Tsuji, H., Hidaka, M., Miyaji, T., Watanabe, T., and Massey, V. (2000) *Journal of Bacteriology* **182**, 5046-5051

77. Wood, Z. A., Poole, L. B., Hantgan, R. R., and Karplus, P. A. (2002) *Biochemistry* **41**, 5493-5504

78. Wood, Z. A., Poole, L. B., and Karplus, P. A. (2001) *Biochemistry* **40**, 3900-3911

79. Poole, L. B., Godzik, A., Nayeem, A., and Schmitt, J. D. (2000) *Biochemisty* **39**, 6602-6615

80. Wood, Z. A., Poole, L. B., and Karplus, P. A. (2003) *Science* **300**, 650-653

81. Higuchi, M., Shimada, M., Yamamoto, Y., Hayashi, T., Koga, T., and Kamio, Y. (1993) *Journal of General Microbiology* **139**, 2343-2351

82. Choi, H. J., Kang, S. W., Yang, C. H., Rhee, S. G., and Ryu, S. E. (1998) *Nat Struct Biol* **5**, 400-406

83. Wood, Z. A., Schroder, E., Robin Harris, J., and Poole, L. B. (2003) *Trends Biochem Sci* **28**, 32-40

84. Massey, V., and Curti, B. (1966) *The Journal of Biological Chemistry* **241**, 3417-3423

85. Hummel, W., and Riebel, B. (2003) *Biotechnology Letters* **25**, 51-54

86. Bolotin, A., Mauger, S., Malarme, K., Ehrlich, S. D., and Sorokin, A. (1999) *Antoinie Van Leeuwenhoek* **76**, 27-76

87. Higuchi, M., Yamamoto, Y., Poole, L. B., Shimada, M., Sato, Y., Takahashi, N., and Kamio, Y. (1999) *Journal of Bacteriology* **181**, 5940-5947

88. Marty-Teysset, C., de la Torre, F., and Garel, J. (2000) *Appl Environ Microbiol* **66**, 262-267

89. Higuchi, M., Yamamoto, Y., Poole, L. B., Shimada, M., Sato, Y., Takahashi, N., and Kamio, Y. (1999) *J Bacteriol* **181**, 5940-5947

90. Gibson, C. M., Mallett, T. C., Claiborne, A., and Caparon, M. G. (2000) *J Bacteriol* **182**, 448-455

91. Mallett, T. C., and Claiborne, A. (1998) *Biochemistry* **37**, 8790-8802

92. Ross, R. P., and Claiborne, A. (1992) *Journal of Molecular Biology* **227**, 658-671

93. Yeh, J. I., Claiborne, A., and Hol, W. G. (1996) *Biochemistry* **35**, 9951-9957

94. Crane, E. J., 3rd, Parsonage, D., Poole, L. B., and Claiborne, A. (1995) *Biochemistry* **34**, 14114-14124

95. Stehle, T., Ahmed, S. A., Claiborne, A., and Schulz, G. E. (1991) *J Mol Biol* **221**, 1325-1344

96. Beres, S. B., Sylva, G. L., Barbian, K. D., Lei, B., Hoff, J. S., Mammarella, N. D., Liu, M. Y., Smoot, J. C., Porcella, S. F., Parkins, L. D., Campbell, D. S., Smith, T. M., McCormick, J. K., Leung, D. Y., Schlievert, P. M., and Musser, J. M. (2002) *Proc Natl Acad Sci U S A* **99**, 10078-10083

97. Kuriyan, J., Krishna, T. S., Wong, L., Guenther, B., Pahler, A., Williams, C. H., Jr., and Model, P. (1991) *Nature* **352**, 172-174

98. Karplus, P. A., and Schulz, G. E. (1987) *J Mol Biol* **195**, 701-729

99. Waksman, G., Krishna, T. S., Williams, C. H., Jr., and Kuriyan, J. (1994) *J Mol Biol* **236**, 800-816

100. Zhang, Y., Bond, C. S., Bailey, S., Cunningham, M. L., Fairlamb, A. H., and Hunter, W. N. (1996) *Protein Sci* **5**, 52-61

101. Lountos, G. T., Riebel, B. R., Wellborn, W. B., Bommarius, A. S., and Orville, A. M. (2004) *Acta Crystallogr D Biol Crystallogr* **60**, 2044-2047

102. Hoefnagel, M. H. N., Starrenburg, M. J. C., Martens, D. E., Hugenholtz, J., Kleerebezem, M., Swam, I. I. V., Bongers, R., Westerhoff, H. V., and Snoep, J. L. (2002) *Microbiology* **148**, 1003-1013

103. Massey, V. (2000) *Biochemical Society Transactions* **28**, 283-296

104. Saeki, Y., Nozaki, M., and Matsumoto, K. (1985) *Journal of Biochemistry* **98**, 1433-1440

105. Park, H. J., Reiser, C. O. A., Kondruweit, S., Erdmann, H., Schmid, R. D., and Sprinzl, M. (1992) *European Journal of Biochemistry* **205**, 881-885

106. Koike, K., Kobayashi, T., and Sato, S. (1985) *Journal of Biochemistry* **97**, 1279-1288

107. Breuer, M., Ditrich, K., Habicher, T., Hauer, B., Kebeler, M., Sturmer, R., and Zelinski, T. (2004) *Angew Chem Int Ed Engl* **43**, 788-824

108. Ogawa, J., and Shimizu, S. (2002) *Curr Opin Biotechnol* **13**, 365-375

109. Appel, D., Lutz-Wahl, S., Fischer, P., Schwaneberg, U., and Schmid, R. D. (2001) *J Biotechnol* **88**, 167-171

110. Wolberg, M., Hummel, W., Wandrey, C., and Muller, M. (2000) *Angew Chem Int Ed Engl* **112**, 4476-4478

111. Yasohara, Y., Kizaki, N., Hasegawa, J., Wada, M., Kataoka, M., and Shimizu, S. (2001) *Tetrahedron: Asymmetry* **12**, 1713-1718

112. Haberland, J., Hummel, W., Daubmann, T., and Liese, A. (2002) *Org. Proc. Res. Dev.* **6**, 458-462

113. Haberland, J., Kriegesmann, E., Wolfram, E., Hummel, W., and Liese, A. (2002) *Org. Proc. Res. Dev.* **6**

114. Anderson, B. A., Hansen, M. M., Harkness, A. R., Henry, C. L., Vicenzi, J. T., and Zmijewski, J. (1995) *Journal of the American Chemical Society* **117**, 12358-12359

115. Cull, S. G., Holbrey, J. D., Vargas-Mora, V., Seddon, K. R., and Lye, G. J. (2000) *Biotechnol Bioeng* **69**, 227-233

116. Howarth, J., James, P., and Dai, J. F. (2001) *Tetrahedron Letters* **42**, 7517-7519

117. Kragl, U., Eckstein, M., and Kaftzik, N. (2002) *Curr Opin Biotechnol* **13**, 565-571

118. Matsuda, T., Harada, T., and Nakamura, K. (2000) *Chemistry Communication*, 1367-1368

119. Wermuth, B. (1992) *Prostaglandins* **44**, 5-9

120. Krook, M., D. Ghosh, Duax, W., and Jornvall, H. (1993) *FEBS Letter* **322**, 139-142

121. Wermuth, B. (1985) *Biol. Res.* **174**, 209-230

122. Forrest, G. L., and Gonzalez, B. (2000) *Chemico-Biological Interactions* **129**, 21-40

123. Baker, M. E. (1994) *Biochem. J.* **300**, 605-607

124. Zelinski, T., Peters, J., and Kula, M. R. (1994) *J. Biotechnol.* **33**, 283-292

125. J. Peters, T. Minuth, and Kula, M. R. (1993) *Enzyme Microb. Technol.* **15**, 950-958

126. Oppermann, U. C., Nagel, G., Belai, I., Bueld, J. E., Genti-Raimondi, S., Koolman, J., K.J. Netter, and Maser, E. (1998) *Chem. Biol. Interact.* **114**, 211-224

127. G. Guan, M. Tanaka, T. Todo, G. Young, M. Yoshikuni, and Nagahama, Y. (1999) *Biochem. Biophys. Res. Commun* **255**, 123-128

128. H. Jornvall, B. Persson, M. Krook, S. Atrian, R. Gonzalez-Duarte, J. Jeffery, and D. Ghosh. (1995) *Biochemistry* **34**, 6003-6013

129. Kizaki, N., Yasohara, Y., Hasegawa, J., Wada, M., Kataoka, M., and Shimizu, S. (2001) *Applied Microbiological Biotechnology* **55**, 590-595

130. Yasohara, Y., Kizaki, N., Hasegawa, J., Takahashi, S., Wada, M., Kataoka, M., and Shimizu, S. (1999) *Applied Microbiological Biotechnology* **51**, 847-851

131. Yamamoto, H., Mitsuhashi, K., Kimoto, N., Matsuyama, A., Esaki, N., and Kobayashi, Y. (2004) *Bioscience Biotechnology and Biochemistry* **68**, 638-649

132. Kataoka, M., Yamamoto, K., Kawabata, H., Wada, M., kita, K., Yanase, H., and Shimizu, S. (1999) *Applied Microbiological Biotechnology* **51**, 486-490

133. Kataoka, M., Hoshino-Hasegawa, A., Thiwthong, R., Higuchi, N., Ishige, T., and Shimizu, S. (2005) *Applied Microbiological Biotechnology*

134. Galkin, A., Kulakova, L., Yoshimura, T., Soda, K., and Esaki, N. (1997) *Applied and Environmental Microbiology* **63**, 4651-4656

135. Bommarius, A. S., Schwarm, M., and Drauz, K. (1996) *Chimica Oggi* **14**, 61-64

136. Bommarius, A., and Riebel, B. R. (2004) *Biocatalysis: Fundermentals and applications*, 549-556

137. Bommarius, A. S., Drauz, K., Klenk, H., and Wandrey, C. (1992) *Ann N Y Acad Sci* **672**, 126-136

138. H. Schutte, J. Flossdorf, H. Sahm, and Kula, M.-R. (1976) *Eur. J. Biochem.* **62**, 151-160

139. Wedy, M. (1992) *Reaction Engineering and Control Investigation*

140. Dalzile, K., and Dickinson, F. M. (1966) *Biochem J.* **100**, 491

141. St Clair, N., Wang, Y. F., and Margolin, A. L. (2000) *Angewandte Chemie* **39**, 380-383

142. Dickinson, F. M., and Dalziel. (1967) *Nature* **214**, 31-33

143. Adolph, H. W., Patrik Maurer, Helga Schneider-bernlohr, Sartorius, C., and Zeppezauer, M. (1991) *Eur J Biochem* **201**, 615-625